Autoimmunity to hypocretin and molecular mimicry to flu antigens in Type 1 narcolepsy

Guo Luo[1], Aditya Ambati[1†], Ling Lin[1†], Mélodie Bonvalet[1], Markku Partinen[2], Xuhuai Ji[3], Holden Terry Maecker[3], Emmanuel Jean-Marie Mignot[1*]

[1] Center for Sleep Sciences and Medicine, Stanford University School of Medicine, Palo Alto CA 94304, USA.

[2]Helsinki Sleep Clinic, Vitalmed Research Centre, Helsinki, Finland and Department of Clinical Neurosciences, University of Helsinki, Helsinki, Finland.

[3]Immune Monitoring Center, Institute for Immunity, Transplantation, and Infection, Stanford University School of Medicine, Palo Alto, CA 94305, USA.

†: Equally contributing second authors

*Correspondence should be addressed to: Emmanuel Mignot, Director, Center For Sleep Sciences and Medicine, 3165 Porter Drive, #2178, Palo Alto CA 94304, USA. (1)650-725-6517 (tel), (1)650-725-7341 (fax), mignot@stanford.edu.

Abstract

Type 1 narcolepsy (T1N) is caused by hypocretin (HCRT) neuronal loss. Association with the Human Leukocyte Antigen (HLA)-DQB1*06:02/DQA1*01:02 (98% vs 25%) heterodimer (DQ0602), T cell receptor (TCR) and other immune loci suggest autoimmunity but autoantigen(s) are unknown. Onset is seasonal and associated with influenza A, notably pandemic 2009 H1N1 (pH1N1). An extensive unbiased DQ0602 binding peptide screen was performed encompassing peptides derived from Pandemrix® X-179-A pH1N1 influenza-A vaccine, a known T1N trigger, other H1N1 strains, and potential human autoantigens HCRT and RFX4, identifying 109 binders. The presence of cognate tetramer-peptide specific $CD4^+$ T cells was studied in 35 narcolepsy cases and 22 DQ0602 controls after expansion of antigen-specific cells in Peripheral Blood Monocytes Cell (PBMC) cultures. Higher reactivity to influenza epitopes $pHA_{273-287}$ (pH1N1 specific) and PR8 (H1N1 pre 2009)-specific NP_{17-31} were observed in T1N. Extensive reactivity to C-amidated but not native version of $HCRT_{54-66}$ and $HCRT_{86-97}$, which are two highly homologous peptides ($HCRT_{NH2}$) was observed with higher frequencies of specific T cells in T1N. TCRα/β CDR3 sequences found in $pHA_{273-287}$, NP_{17-31} and $HCRT_{NH2}$ tetramer positive $CD4^+$ cells were also retrieved in single INFγ-secreting $CD4^+$ sorted cells stimulated with Pandemrix®, confirming immunodominance and functional significance in DQ0602-mediated responses and molecular mimicry. TCRα/β CDR3 motifs of $HCRT_{54-66}$ and $HCRT_{86-97}$ tetramers were extensively shared. Particularly notable was sharing across subjects of an CDR3α, CAVETDSWGKLQF (in association with various CDR3β), that used TRAJ24, a chain modulated by Single Nucleotide Polymorphism (SNPs) rs1154155 and rs1483979 associated with T1N. Sharing of

CDR3β CASSQETQGRNYGYTF (in association with various CDR3α) was also observed with $HCRT_{NH2}$ and $pHA_{273-287}$-tetramers across subjects. This segment uses TRBV4-2, a segment modulated by narcolepsy-associated SNP rs1008599. Higher $HCRT_{NH2}$ positive $CD4^+$ T cell numbers in T1N together with sharing of J24 CAVETDSWGKLQF in $HCRT_{NH2}$ autoimmune responses, indicates causal DQ0602-mediated $CD4^+$ autoreactivity to HCRT in T1N. Our results provide evidence for autoimmunity and molecular mimicry with flu antigens modulated by genetic components in the pathophysiology of T1N.

Main text

Whereas genetic[1-6], epidemiological[7-11] and pathophysiological[12-14] studies implicate autoimmunity in response to flu infection in type 1 narcolepsy (T1N), a disease caused by hypocretin (HCRT) neuronal loss[15-17], the identity of the autoantigen is unknown. Potential autoantigens explored have included HCRT sequences[18-21], HCRT receptor 2 sequences[22] and the protein TRIB2[23] but these results have either been withdrawn[24] or not replicated[25-27]. Similarly, staining of hypothalamic slices with T1N sera has been found negative[28].

Leading on from prior work[1-6] a large recent GWAS analysis of over 4,500 patients across multiple ethnic groups confirmed primordial importance of the Human Leukocyte Antigen (HLA) DQ0602 heterodimer in disease predisposition, with important secondary associations in T cell receptor (TCR) loci α and β and other immune loci such as perforin. This suggests importance of DQ0602 presentation of antigens to $CD4^+$ by Antigen Presenting Cells (APC) and likely subsequent $CD8^+$ destruction of hypocretin cells[29]. Hypocretin cell cytotoxicity through $CD4^+$ and $CD8^+$ mediation has also been shown to cause narcolepsy in an animal model[30].

Recently, much has recently been learned regarding what may trigger T1N autoimmunity. Onset of T1N in children, which can often be timed to the week, is seasonal and peaks in spring and summer[10]. Onset has also been associated with Streptococcus Pyogenes infections[9,31] and Influenza-A[10], suggesting the trigger may be a winter infection, followed by a delay peaking at 5 months once sufficient hypocretin cell loss has occurred and

symptoms appear. Most strikingly, prevalence of T1N increased severalfold in China with a similar delay following the 2009-2010 “Swine Flu” H1N1 influenza pandemic (pH1N1)[10,32,33], however, association with the pandemic is less clear in other countries[11,34]. Similarly, cases of T1N have been triggered by Pandemrix® in Europe with relative risk increasing 5 to 14-fold in children and adolescents and 2 to 7-fold in adults after vaccination[33]. As Pandemrix® is an AS03 adjuvanted vaccine containing the artificially produced reassortant strain X-179A, a mix of PR8, an old H1N1 strain derived from pre-2009 seasonal H1N1 but containing key H1N1 2009 surface proteins (Hemagglutinin-HA and Neuraminidase-NA)[35], flu proteins are likely to be critically involved. The fact that HLA and TCR genetic associations are universal[6,36-40] is also consistent with a flu trigger, as Influenza-A infections occur on gobal basis[41]. Importantly, however, even with Pandemrix® vaccination in Europe, only 1 in 16,000 vaccinated children developed T1N. As has been illustrated above, both the H1N12009 pandemic and the Pandemrix® vaccination have exibited variable effects across different countries, thus demanding the consideration of additional factors to fully explain T1N occurences.

Results

DQ0602 restricted epitopes of H1N1 flu responses in T1N versus controls suggest a role for $pHA_{273-287}$ and NP_{17-31}

Complementing our previously published data[18,24], we screened overlapping 15-mers for DQ0602 binding for key proteins contained in X-179A and pH1N1 wild type, HA, NA, Influenza RNA-dependent RNA polymerase subunit 1 (PB1) and nucleoprotein (NP)

(Supplementary Table 1). HA and NA were selected as these are key surface proteins enriched by design in flu vaccines such as Pandemrix® (to facilitate B cell responses)[35,42]. PB1 was selected because it is of H1N12009 origin in Pandemrix® and thus is also shared by the wild type H1N12009 virus and Pandemrix®, two known triggers of T1N[35,42]. We further added NP to our screen as it is the most abundant protein in flu and it is also present in large amounts in Pandemrix® as enrichment process for surface proteins is not absolute in this vaccine (and many others, although some subunit specific vaccine were available, such as Focetria® for pH1N1)[35]. NP of Pandemrix® is of backbone PR8 origin[35,42]. Screening was primarily done using A/reassortant/NYMC X-179A (California/07/2009 x NYMC X-157, reference ADE2909) sequences complemented by wild type pH1N1 sequence (A/California/07/2009, reference AFM728) when polymorphism was evident, or sequences are of distinct origin (i.e. NP). Screening for these proteins identified large number of binders (Supplementary Table 1) using the biotin-conjugated $EBV_{486–500}$ epitope (Bio-EBV, Bio-GGGRALLARSHVERTTDE), a known binder[18,43]. Peptides that outcompeted >75% of the reference EBV peptide signal were considered binders, and these were selected for tetramer screening[18,24].

To assess for the presence of $CD4^+$ T cells reactive to these epitopes, likely 9 mer-MHC class II binding repertoires were determined for all binders using three Immune Epitope Database prediction algorithms (SMM_align, NN_align, and consensus) and similarity scores. Peptides (15-mers) surrounding the cores and displacing most of the bio-EBV peptide in competition assays were used to construct tetramers by peptide exchange using biotinylated DQ0602 (Bio-DQ0602) cleaved with thrombin as described in the

methods section. These tetramers were then used to FACS stain 10-day expanded peripheral blood mononuclear cells (PBMCs) cultures of 6 cases and 4 DQ0602 controls stimulated with Pandemrix® (100 ng/ml) or the corresponding single peptide (6.25 μM) (see methods and staining results in Extended Data Figure 1a). The control and narcoleptic subjects were all known post Pandemrix® vaccinees except for one case who developed T1N independent of vaccination 6 months prior to blood sampling (recent onset case).

Figure 1a shows the number of controls and T1N patients (from 10 subjects) positive for each tetramer staining as well as example staining (Figure 1d) with selected tetramers. Tetramer positivity ranged from no positive to 10 positives for some tetramers (Figure 1a), with mean number of positives per flu protein in post Pandemrix® controls (4) and T1N (5) cases shown in Figure 1c. Post Pandemrix® cases and controls were selected for Figure 1c comparison to ensure similar flu antigen exposure and as expected no difference was found across cases and controls for these antigens overall (all epitopes). In contrast, lower reactivity with PB1 versus HA, NP and NA was found, likely the consequence of the lower concentration of PB1 in the Pandemrix® vaccine (and all vaccines) in comparison to these other proteins[35].

X179A derived tetramers with the most staining included $pHA_{273-287}$, $pNA_{217-231}$, NP_{17-31}, $NP_{261-275}$ (Figure 1d) suggesting these epitopes are immunodominant (Figure 1a, NP epitopes from pH1N1 instead of PR8 indicated by stars). Other immunodominant peptides include $pHA_{209-223}$, $pHA_{321-335}$, $pHA_{437-451}$, pNA_{45-59}, $pNA_{217-231}$, $NP_{261-275s}$ (shared

epitope between pH1N1 and PR8), and $NP_{437-451-pH1N1}$*. $pHA_{273-287}$ is notable as it was previously reported to have homology with prepro-hypocretin sequences $HCRT_{54-66}$ and $HCRT_{86-97}$ and suggested be involved in a possible pathogenic mimicry using Enzyme-Linked ImmunoSpot (ELISpot) results, a publication that was retracted based on flawed ELISpot results (DQ0602 binding results were all verified)[18,24]. Interestingly, among immunodominant epitopes, responses to three epitopes $pHA_{273-287}$ (of H1N12009 origin), NP_{17-31}, and $NP_{261-275}$ (of PR8 origin) were stronger in Pandemrix® vaccinated patients versus controls and positive in the early onset cases (Figure 1a) and were thus selected for additional investigation.

Additional analysis of 24 cases and 14 DQ0602 positive controls confirmed significant overabundance of T cells positive for $pHA_{273-287}$ and NP_{17-31} but not $NP_{261-275}$ (Figure 2a and 2c, Extended Data Figure 1b and Extended Data Figure 2) suggesting that these two epitopes could be involved in the recruitment of differential $CD4^+$ T cell populations related to T1N. Sub-analyses confirmed that these epitopes also gave significantly more response in a total of 11 post-Pandemrix® cases (mean age 17±2yo) versus 8 post-Pandemrix® controls (27±6 yo), an important control as these subjects had a more similar exposure to pH1N1 around the first wave of the pH1N1 pandemic infection (Extended Data Figure 2d). Findings with $pNA_{217-231}$, $NP_{261-275}$ and $NP_{17-31-pH1N1}$, the homologous sequence of PR8 NP_{17-31} in pH1N1 (2 amino acid difference in the core, see Supplementary Table 2) showed no differences overall and in subgroups (Extended Data Figure 2a-c). This demonstrates that increased flu reactivity in T1N versus controls is not broadly shared across all H1N1 epitopes, confirming screening results (Figure 1c).

Broad CD4$^+$ T cell autoreactivity to amidated HCRT$_{54-66-NH2}$ and HCRT$_{86-97-NH2}$ fragments when presented by DQ0602

We next tested whether T1N was associated with autoreactivity involving two proteins known to be primarily co-localized with hypocretin, hypocretin itself and RFX4, a transcription factor primarily expressed in testis and also exceptionally abundant in hypocretin cells[44]. Hypocretin and RFX4 binders were tested in the 10 subjects mentioned above, with results suggesting almost no or little cross reactivity, consistent with T cell tolerance toward autoantigen peptide sequences (Figure 1a-b). Autoreactivity was significantly lower than for all viral proteins (Figure 1c).

Because the pre-prohypocretin peptide is cleaved and post-translationally modified in the region where homologous sequences HCRT$_{54-66}$ and HCRT$_{86-97}$ are located (resulting in secreted hypocretin-1 and -2), most notably C-amidated, a transformation necessary to its biological activity, we also tested HCRT$_{54-66-NH2}$ and HCRT$_{86-97-NH2}$, modified peptides we have previously shown also bind DQ0602 with similar or higher affinity[18]. To our surprise, T cell reactivity to these fragments was high in both DQ0602 controls and T1N subjects (Figure 2b and Extended Data Figure 1). Of notable interest was the fact HCRT$_{54-66-NH2}$ staining was generally restricted to distinct populations (not unlike what was observed with flu antigens) while HCRT$_{86-97-NH2}$ staining was more heterogeneous, suggesting large amounts of low affinity tetramer cross-reactivity (Figure 2d and Extended Data Figure 1). These data were later expanded to 29 cases and 21 DQ0602 positive controls, and a significantly higher ($p=0.0013$) percentage of HCRT$_{54-66-NH2}$ tetramer

positive cells was found in T1N (Figure 2b), with marginally higher values for $HCRT_{86-97-NH2}$ (p=0.056). Sub-analysis of 13 post-Pandemrix® cases (mean age 17±1yo) versus 10 post-Pandemrix® controls (mean age 27±6 yo) confirmed significantly higher reactivity (p=0.0052) for $HCRT_{86-97-NH2}$ and marginally higher values for $HCRT_{54-66-NH2}$ (p=0.067) (Extended Data Figure 2f). Even more strikingly, in 7 recent onset cases (22±6 yo) versus 21 controls (23±3yo) higher reactivity was found to both $HCRT_{54-66-NH2}$ and $HCRT_{86-97}$ (non-amidated) suggesting an important role in the cause of T1N (Extended Data Figure 2g).

T Cell receptor sequencing of flu tetramer positive cells indicate bias in TCRα/β usage consistent with *in-vitro* clonal expansion

Tetramer-reactive $CD4^+$ T cells from 14-20 subjects were next FACS single sorted and sequenced in control and T1N patients (including the 11-13 post Pandemrix® subjects and one early onset case mentioned above) for $pHA_{273-287}$, NP_{17-31}, $HCRT_{54-66-NH2}$ and $HCRT_{86-97-NH2}$. Sporadic additional sequencing (a few subjects, data not shown) was performed for other epitopes. Subjects sequenced are denoted in red in Figure 2a and 2b. For comparison, ~10^6 peripheral memory $CD4^+$ T cells of the same subjects were sequenced for TCRα and TCRβ V and J segment baseline usage (data from: Ollila et al. [29]).

As expected, we found strong significant bias in TCRα/β usage (mostly for TRAV and TRBV segments) specific of each epitope, except for $HCRT_{54-66-NH2}$ and $HCRT_{86-97-NH2}$ where a large amount of sequence sharing was found across the two highly homologous

HCRT epitope (also called $HCRT_{NH2}$ as a group for future reference) and sequence usage diversity was higher in comparison to flu epitopes (Extended Data Figure 3, Supplementary Table 3). For example, TCRα usage of $pHA_{273-287}$ was notable for a most highly significant enrichment in TRAJ23 (Mantel Haenszel [MH] OR=13.6),TRAV13-1 (OR=5.4) and TRAV35 (OR=19.3) while TCRβ usage for the epitope was enriched in TRBV19 (OR=22.4) and TRBV4-3 (OR=35.3) in comparison to the same subject's CD4+ cell peripheral usage, without differences in control versus T1N. Similarly, NP_{17-31} positive TCR cells were enriched in TRAV12-2 (OR=18.3), TRAV8-6 (OR=6.7), TRBV4-2 (OR=25.6), TRBV7-9 (OR=2.8), TRBV20-1(OR=4.7) (Extended Data Figure 3, Supplementary Table 3) without differences in control versus T1N. Of particular interest was enrichment in TRBV4-2, as T1N is strongly associated with rs1008599G (OR=0.81, $p=6.63\ 10^{-12}$), a SNP that is the main eQTL for increased expression of this segment [29,45].

T Cell receptor sequencing of C-amidated HCRT tetramer positive cells indicate broad TCR reactivity and has consequently more limited bias in TCRα/β usage

Sequencing of amidated-HCRT positive tetramers gave a different picture (Extended Data Figure 3, Supplementary Table 3) in comparison to flu-positive tetramer. First, although increased usage of specific TCR segments was found, usage diversity was much higher (Extended Data Figure 3), notably when $HCRT_{86-97-NH2}$ tetramers were used, giving a typically less distinct population with likely lower TCR affinity (Figure 2d, Extended Data Figure 1). In addition, in cases where $HCRT_{54-66-NH2}$ and more rarely $HCRT_{86-97-NH2}$ tetramers gave a clearly separated population on FACS plots (Extended Data Figure 1), sequencing resulted in almost pure oligoclonality of TCR sequences (even

less diverse than with flu antigens) with minimal usage sequence sharing (patients 022, 948, 051 and 685 for $HCRT_{54-66-NH2}$ and controls 567 and 391 for $HCRT_{86-97-NH2}$ in Extended Data Figure 3, with corresponding FACS plots in Extended Data Figure 1).

Shared CDR3 analysis and Grouping of Lymphocytes Interactions by Paratopes Hotspots (GLIPH) analysis across flu and $HCRT_{NH2}$ tetramers

$pHA_{273-287}$ and $HCRT_{54-66-NH2}$/$HCRT_{86-97-NH2}$ share weak epitope homology[18,24], a result confirmed using http://tools.iedb.org/cluster/reference/[46], with three Epstein Barr Virus (EBV) sequences as anchor (Figure 3e). Based on this, mimicry has been proposed but not demonstrated[18,24]. To search for mimicry across $pHA_{273-287}$, NP_{17-31}, $HCRT_{54-66-NH2}$ and $HCRT_{86-97-NH2}$, we first analyzed sharing of CDR3α, CDR3β and CDR3α/β pairs across epitopes. Supplementary Table 4 shows cross tabulations of shared sequences across epitopes.

A large number of sequences were shared between $HCRT_{54-66-NH2}$ and $HCRT_{86-97-NH2}$ tetramers across CDR3α (11.8%), CDR3β (9.3%) and both CDR3 α/β (3.6%), a result that is not surprising considering that $HCRT_{54-66-NH2}$ and $HCRT_{86-97-NH2}$ only differ in their N-amidated C-terminal end, L-$_{NH2}$ (hypocretin-1) and M-$_{NH2}$ (hypocretin-2) in P9 of the binding repertoire (Supplementary Table 2). In contrast, $pHA_{273-287}$, a viral epitope which has been suggested to be a mimic of HCRT and has some homology with $HCRT_{54-66-NH2}$ and $HCRT_{86-97-NH2}$ (see Figure 3e) shared very few of the same clones with $HCRT_{54-66-NH2}$ and $HCRT_{86-97-NH2}$, for example only 1.9% and 1.5% for CDR3α, 0.7% and 1.8 % for CDR3β and none and 0.3% (2 instances) for CDR3α/β with $HCRT_{54-66-NH2}$ and $HCRT_{86-}$

$_{97\text{-}NH2}$ respectively. Potential sharing was even lower with $NP_{17\text{-}31}$, which shared a few clones with $pHA_{273\text{-}287}$, and at even lower level with $HCRT_{NH2}$.

To explore differential CDR3 usage per epitopes and across narcolepsy versus control status we also used the Grouping of Lymphocytes Interactions by Paratopes Hotspots (GLIPH)[47] in CDR3βs from $pHA_{273\text{-}287}$, $NP_{17\text{-}31}$ and $HCRT_{NH2}$. A similar bioinformatic motif driven approach was also implemented for CDR3α. Tetramer derived unique CDR3s were compared to a large database of CDR3 sequences derived from bulk sequencing of ~10^6 $CD4^+$ $CD45RA^-$ T cells obtained from the same 35 narcolepsy and 22 DQ0602 control subjects (see Supplementary Table 5 for a list of paratopes significant at the $p<0.05$ False Discovery Rate value for each epitope). Because CDR3β sequences are more unique than CDR3α, more CDR3β than CDR3α paratopes were enriched across all epitopes (Supplementary Table 5). Interestingly, only one particular paratope motif, SQG, standed out as strongly enriched in narcolepsy versus controls in $pHA_{273\text{-}287}$-tetramer positive cells (Supplementary Table 5). This motif is unique to TRBV4-2 and TRBV4-3 and reflected a significant enrichment of a subset of diverse SQG positive unique CDR3β in 6 narcolepsy patients versus 2 controls. Extended Data Figure 4 also show preferential usage of specific aminoacids in tetramers versus control sequences at various length, an analysis that was not revealing beyond the GLIPH analysis. We note that in comparison to bulk sequencing of total CD4+ memory cells, tetramer specifc CDR3β sequences had frequencies ranging from undetectable ($<1/10^7$) to 1 for 10^5 in the same corresponding subject.

Commonly used CDR3α and CDR3β segments observed with $pHA_{273-287}$ and NP_{17-31} tetramers

We next analyzed sharing of CDR3α, CDR3β and CDR3α/β pairs across patients and controls, with all CDR3 found at least twice across subjects (Figure 3). Not surprisingly, sharing of CDR3α was more frequent than sharing of CDR3β and exact CDR3α/β pairs were rarely seen across subjects. Sharing for viral epitope $pHA_{273-287}$ and NP_{17-31} tetramers was as expected from usage preference reported in Extended Data Figure 3 (for example TRAJ23 for $pHA_{273-287}$ CDR3α CAVSPGNNQGGKLIF, CIVRVLTNQGGKLIF, CIVRVATNQGGKLIF and CAAPYNQGGKLIF). Most commonly used segments in most enriched clones were TRAV8-6, TRAJ34, TRBV7-9 and TRBV4-2 for NP_{17-31}. Usage diversity for $pHA_{273-287}$ was biased toward TRAV13-1, TRAV17 and TRBV4-2, with more limited sharing of TRBV for this epitope. We also noted frequent usage of TRAV26-1 CDR3α across all epitopes; DQ0602 is a strong transQTL of TRAV26-1 segment usage, probably because it interacts through its CDR1α with DQ0602[45].

$HCRT_{NH2}$ tetramers most frequently use J24 positive CDR3α CAVETDSWGKLQF

As mentioned above, TRAJ24, TRAJ28 and TRBV 4-2 are of special interest as genetic QTL locations modulating usage of these segments are associated with narcolepsy. While TRAJ28 did not show any particular over representation in our data, we observed extensive sharing of TRAJ24 and TRBV4-2. The most striking finding was extensive sharing of TRAJ24 CDR3α TRAV2-CAVETDSWGKLQF-TRAJ24 patients and controls with $HCRT_{54-66-NH2}$ and $HCRT_{86-97-NH2}$ respectively (Figure 3c and d). As TRAJ24 is a low

usage segment (0.87%), this is highly significant. Supplementary Tables 6 and 7 report on all TRAJ24 and TRBV4-2 positive clones found in all cultures, respectively. We focused on clones containing TRAJ24 CDR3α CAVETDSWGKLQF the major CDR3α shared across patients and controls following $HCRT_{NH2}$ stimulation (Figure 3). All these clones also use TRAV2. As can be seen, the CAVETDSWGKLQF CDR3α generally occurs in the context of diverse CDR3βs containing TRBV15, TRBV2, TRBV29-1, TRBV9 in controls and TRBV15, TRBV3-1, TRBV7-2 and TRBV20-1 in patients. Only TRAV15-CATSSGGGGKAYGYTF CDR3β was shared by 2 patients and one control following $HCRT_{NH2}$ culture and tetramer isolation. Of note, CAVETDSWGKFQF was not observed in any subject, control or T1N. This suggests that TCRβ is less important for interaction of these TCR α/β with $HCRT_{54-66-NH2}$ and $HCRT_{86-97-NH2}$ when presented by DQ0602.

Single cell sorting and TCR sequencing of INFγ positive, Pandemrix® reactive $CD4^+$ T cells confirms the importance of $pHA_{273-287}$ and NP_{17-31} as immunodominant peptides of the HLA class II response to Pandemrix® and suggest mimicry with HCRT $CD4^+$ responses

CarboxyFluorescein Succinimidyl Ester (CFSE)-tagged PBMCs from 8 patients and 8 controls were expanded (overlapping with the sample above) in the presence of Pandemrix® in a 7-day period following which CFSE-low $CD4^+$ cells were sorted and expanded further for a 4day period and then stimulated with autologous monocytes prepulsed with Pandemrix®, following which single cell sequencing of INFγ-positive (Pandemrix®-reactive), CFSE low (having divided in the presence of Pandemrix® during

the culture) $CD4^+$ cells was performed. This experimental design amplifies all Major Histocompatibility Complex (MHC) Class II mediated responses, with DQ0602 mediated responses likely in the minority, notably because DRB1 responses are typically dominant among Class II responses. To limit this problem, one patient repeated twice was also cultured with Pandemrix® in the presence of anti DR and anti DP antibodies. In this case, presentation and reactivity should be limited or enriched for DQ response (DQ0602 and the other trans located allele). Upon completion of these experiments, CDR3 TCRα and TCRβ sequences were matched with tetramer-derived sequences to search for commonality (Supplementary Table 8). Strikingly, we found that $pHA_{273-287}$ and NP_{17-31} tetramer sequences, in many cases sharing both TCRα and β chains were present in these cultures, most notably in the cultures than had been blocked by anti DR and DP antibodies. Interestingly, we also found a significant number of sequences shared with $HCRT_{54-66-NH2}$, $HCRT_{86-97-NH2}$ tetramer sequences suggesting mimicry with one or several unknown peptide variants in Pandemrix®. As a control, no sharing was found with single sorted $CD8^+$ cell TCR sequences reactive to Pandemrix® were isolated using a similar procedure (data not shown).

Selected $pHA_{273-287}$ associated CDR3β are found in $HCRT_{NH2}$ J24 positive CDR3α CAVETDSWGKLQF positive tetramers, with a major node using TRBV4−2 CDR3β CASSQETQGRNYGYTF across $HCRT_{NH2}$ and $pHA_{273-287}$ tetramers. Such connections are not found with NP_{17-31} positive tetramers

In Figure 4, paired CRD3α and CRD3β found in various tetramers across antigens (from Supplementary table 4) were plotted as a network plot, with the thickness of connecting

lines reflecting number of clones found with each denoted heterodimer. Clones found only once across epitopes within the same patient were removed to avoid the possibility of contamination. Tables in Figure 4b-4d indicate key used segments in this connectome. As can be seen, a clearly separated cluster that uses TRBV7-9, TRAV8-6, TRAV6, TRAJ34, and TRBV4-2 was formed with NP_{17-31} (Figure 4d). In contrast, clusters of $HCRT_{NH2}$ and $pHA_{273-287}$ are tightly connected (Figure 4b and 4c), reflecting not only sequence homology between these epitopes and increased sharing of specific CDR3α and CDR3β (Supplementary Table 4) but also revealing two groups of antigen-specific heterodimers ($HCRT_{NH2}$ and $pHA_{273-287}$ -specific) connected through a few discrete likely crossreactive nodes.

The $HCRT_{NH2}$ reactive node is centered around the identified CDR3α TRAV2-CAVETDSWGKLQF-TRAJ24 (Figure 4b). As mentioned above, this TCRα chain connects with a large variety of diverse TCRα sequences, suggesting that $HCRT_{NH2}$ may interact more primarily with TCRα. Other $HCRT_{NH2}$ nodes, such as TRBV2 CASSGAGGFYNEQFF, TRBV3 CASSQGGTYRETQYF and TRAV12-2 CAVNIDGGYQKVTF TRAVJ23 are connected to it.

$pHA_{273-287}$ reactive nodes are multiples and include: CDR3β TRBV4−2 CASSQETQGRNYGYTF, TRBV15 CATSSGGGGKAYGYTF, TRBV18 CASSPTGRPQETQYF, CDR3α TRAV13-2 CAENYGAGGTSYGKLTF TRAJ52 and TRAV26-1 CIVRSQGGSYIPTF TRAJ6 among others. Presumably TCR α/β containing these chains have high affinity for $pHA_{273-287}$ in various combinations.

Most interestingly, $pHA_{273-287}$ and $HCRT_{NH2}$ positive nodes join in several places through less frequent heterodimers that also use the primary $HCRT_{NH2}$ CDR3α TRAV2-CAVETDSWGKLQF-TRAJ24. These include $HCRT_{NH2}$ reactive CDR3βs: TRBV15 CATSRDTMTSIGTDTQYF (2 clones in 2 controls), TRBV4−2 CASSQETQGRNYGYTF (one clone in one patient) and TRBV4-3 CASSQGNTGHSPLHF (one clone in one control) and TRBV4-3 CASSQGDVNYGYTF (one clone in one control)) (see supplementary Table 5 and 6). These CDR3βs are used by other heterodimers with distinct CDR3αs in the context of $pHA_{273-287}$. Of further interest is the fact that CDR3β TRBV4-2-CASSQETQGRNYGYTF is paired with CRD3α TRAV13-1-CAASDNDMRF-TRAJ43 (25 occurrences in one subject) in the context of $pHA_{273-287}$, indicating it is an important heterodimer for this response. Of note, one direct connection between TRAV2 CAVETDSWGKLQF TRAJ24 and TRBV20-1 CSASPLGRGTEAF (17) primarily used by NP_{17-31} is also present, suggesting that some limited mimicry could also occur with NP_{17-31}. Other connections are occurring through CDR3α, which are generally less antigen specific.

Discussion

In this work, we screened two potential autoantigens for DQ0602 binding and T cell reactivity using tetramer staining of PBMCs of T1N cases and controls. Hypocretin and RFX4 were selected because of their high enrichment in hypocretin cell[44]. RFX4 is interesting because of its primary expression in testis and its involvement in midline brain development[48]. Furthermore, the only known established autoimmune disease with

secondary hypocretin cell loss is anti-Ma2 encephalitis, a disease associated with seminomas and $CD8^+$ T-mediated destruction of hypocretin cells[49]. We found only limited TCR reactivity directed towards any segment of the native HCRT peptide sequence (or RFX4), but strong reactivity to the N-Amidated, post-translationally modified (PTM) C-terminal end of hypocretin-1 and 2 (denoted $HCRT_{54\text{-}66\text{-}NH2}$ and $HCRT_{86\text{-}97\text{-}NH2}$ or, as a group, as $HCRT_{NH2}$) (Figure 1). The two peptides, also called orexin-A and orexin –B, are homologous peptides that differ only in their C-terminal amidated residue, L- $_{NH2}$ for orexin-A and M- $_{NH2}$ for orexin B.. These are secreted by hypocretin neurons after undergoing amidation of their C-terminal end, a PTM necessary for biological activity[50]. The observation of higher reactivity of $HCRT_{NH2}$ extends other observations made in other autoimmune diseases, such as Rheumatoid Arthritis, Celiac disease and Type 1 Diabetes[51], indicating that PTMs are frequently present in autoantigens. The current explanation is that PTMs do not occur sufficiently in the thymus during central tolerance establishment[52], and thus increase the risk of autoimmunity.

Relevant to T1N, we also found that patients have higher numbers of $CD4^+$ T cells binding $HCRT_{54\text{-}66\text{-}NH2}$ when presented by DQ0602, the major HLA allele associated with T1N (97% versus 25% in controls) (Figure 2). Recent onset cases also showed significantly higher numbers of T cells recognizing $HCRT_{86\text{-}97\text{-}NH2}$, a peptide differing only in its C-terminal amino-acid from $HCRT_{54\text{-}66\text{-}NH2}$. These results indicate that autoreactivity to amidated $HCRT_{NH2}$ fragments is common in both patients and controls but occurs at higher levels in patients. These findings are consistent with other publications reporting occasional cross-reactivity to HCRT in both patients and controls, although these studies

used ELISpots in a small number of samples, finding no differences by disease status[19,20]. The findings above could reflect causality, cross-reactivity secondary to hypocretin cell loss via another mechanism, or an epiphenomenon. Strikingly however, not only was sharing of CDR3 sequences found across patients (as recently reported for gluten-reactive T cells in Celiac Disease[53]) but the top CDR3α CAVETDSWGKLQF involved in the recognition of $HCRT_{NH2}$ in controls and patients uses TRAJ24 (Figure 3), a segment marked by SNPs rs1154155G and rs1483979 strongly associated with T1N risk[6]. This genetic association is the strongest association after HLA across all ethnicity[1-6] and as TRAJ24 is normally only used rarely (0.8% of repertoire)[29], the result must indicate causality. In addition to that, we found common sharing of CDR3β TRBV4-2 CASSQETQGRNYGYTF in cases and controls with $HCRT_{NH2}$ and $pHA_{273-287}$ across 4 subjects (Figure 3, Supplementary Table 4) . This is likely to be functionally significant as TRVB4-2 is also rarely used (0.7% of repertoire)[29], and expression of this segment is linked with narcolepsy-associated SNP rs1008599[6,29,45].

Considering these associations, our data indicate that T1N is caused by autoimmunity to $HCRT_{NH2}$ either through dysregulation of regulatory T cells or through increased pathogenicity of the TRAJ24F allele. Because controls have the same CDR3α however, it is likely not sufficient in itself to escalate to full hypocretin cell loss and establishment of the T1N phenotype. Additional phenotyping of autoreactive cells carrying CDR3α CAVETDSWGKLQF will be required in order to answer these questions, together with $CD8^+$ T cell studies. Genetic[29] and animal studies[30] indeed suggest a $CD4^+$ helper

$CD8^+$ cytotoxic model as the most likely to explain hypocretin cell loss in T1N, although involvement of cytotoxic $CD4^+$ T cells is also possible.

Furhermore, we demonstrate that T1N is associated with differential reactivity to at least two flu peptides, $pHA_{273-287}$ and NP_{17-31}, derived from X-179A, the reassortant strain used in Pandemrix® (Figure 2). This vaccine has been linked with T1N onset in Northern Europe[34], however the latter correlation varies across countries[34], suggesting interactions with other factors. Of particular interest was the fact that one peptide, $pHA_{273-287}$, is specific of 2009H1N1, while another peptide $NP_{17-31,}$ is specific of the vaccine backbone strain PR8, an old seasonal H1N1 strain originally derived from 1918H1N1. The NP_{17-31} sequence is representative of seasonal H1N1 prior to the 2009 pandemic flu, a strain currently circulating at a lower frequency. Whether or not involved in mimicry, our data also suggest that flu epitopes derived from multiple H1N1 strains (pH1N1, PR8-like) may be needed to favour immune response towards T1N immunity, and that overall homology between HCRT and flu sequences may be of greater importance. If this was the case, a particular history of coincident flu infections, together with specific past exposure, could preferentially trigger T1N, explaining why the H1N12009 pandemic may have led to a more compelling increase of T1N in China[10,33] as supposed to other countries. Influenza-A creates low fidelity copies and mutates in vivo during the course of infections or in specific vaccines, which could also contribute to rare mutated epitope exposure in some cases[35,54]. In this context, Pandemrix® vaccination coincidental with pH1N1 pandemic or other strains may have been a perfect storm in some countries. The confluence of exposure to multiple epitopes could also explain why the administration of Arepanrix® ,

an adjuvanted vaccine similar to Pandemrix® which was used in Canada, has not exhibited a strong link to T1N[55].

$pHA_{273-287}$ has significant homology with $HCRT_{54-66}$ and $HCRT_{86-97}$ sequences and their binding repertoire[18], making it a suitable mimicry candidate with $HCRT_{NH2}$ (Figure 3). This is reflected by increased sharing of CDR3α and CDR3β sequences in the corresponding tetramers, that was high within $HCRT_{NH2}$ peptides, substantial between $HCRT_{NH2}$ and $pHA_{273-287}$ but almost absent between $HCRT_{NH2}$ and NP_{17-31} or between $pHA_{273-287}$ and NP_{17-31} (Supplementary Table 4). This almost linear relationship suggests the more homology the mimic has with the autoantigen sequence, the most likely similar TCR sequences are recruited by crossreactivity. Surprisingly however, the number of epitope-specific GLIPH paratopes shared between sequences was similar. We also tried to examine whether TCR paratope motifs common to $HCRT_{NH2}$ and $pHA_{273-287}$ recognition were more abundant in $HCRT_{NH2}$ positive tetramers from patients versus controls, however no compelling observations were made (data not shown).

Most revealing was a network analysis examining CDR3α and CDR3β sharing across $pHA_{273-287}$, NP_{17-31} and $HCRT_{NH2}$ tetramers (Figure 4). In this analysis, clearly separate clusters of connected CDR3α–CDR3β heterodimers emerged for NP_{17-31} tetramers and a subset of $pHA_{273-287}$ heterodimers. In addition to this, a large $HCRT_{NH2}$ tetramer cluster centered around CDR3α TRAV2 CAVETDSWGKLQF TRAJ24 was formed, but it was also connected to two strongly expressed $pHA_{273-287}$ heterodimer nodes through $HCRT_{NH2}$ CDR3β TRBV4−2 CASSQETQGRNYGYTF in one patient, and TRBV15

CATSRDTMTSIGTDTQYF, TRBV4-3 CASSQGNTGHSPLHF or CASSQGDVNYGYTF in a few controls (see supplementary Table 5 and 6 and Figure 4). This result is remarkable as narcolepsy is genetically associated with SNPs that regulate usage of two of these three segments, TRAJ24 and TRBV4-2, suggesting causality. For the other two connections, TRBV15 and TRBV4-3, examination of Quantitative Ttrait Loci (QTL) effects for these segments did not reveal any genomic effect[29] unlike the well-established TRBV4-2 effect[29,45], thus functional connection through genetic association could not be tested. Of particular interest is the size of the TRAV26-1 CIVRSQGGSYIPTF CDR3α node, likely explained by the fact that TRAV26-1 is a transQTL for DQ0602, reflecting direct CDR1/2 interactions of TRAV26-1 with the DQ0602 molecule, notably DQβ, the most specific portion of the DQ molecule[45].

In the case of TRBV4-2, the connection is direct, as narcolepsy-associated SNP rs1008599A increases usage of this segment, and thus presumably the risk of the crossreactive CDR3α TRAV2 CAVETDSWGKLQF TRAJ24 / CDR3β TRBV4−2 CASSQETQGRNYGYTF heterodimer to occur. For TRAJ24, the connection is more complex as the genetic signal encompasses several SNPs (notably rs1154155G and rs1483979C), one of which changes an aminoacid within TRAJ24, so that its terminal CDR3α end region is GKFQF instead of GKLQF (L is the most common allele in Caucasians). In addition to this effect, narcolepsy-associated SNPs also decrease TRAJ24 expression and increase TRAJ28 expression (a segment not involved in our dataset). In our dataset, the major narcolepsy-associated CDR3α segment observed is TRAV2 CAVETDSWGKLQF TRAJ24, as segment containing the L allele that is protective

for narcolepsy. TRAV2 CAVETDSWGKFQF TRAJ24 was not observed. This could be explained by the fact TRAJ24F is expressed at about half the level of TRAJ24L[29] and is only present in 30% of our patients tested, most of whom are J24 L/L homozygous (the most frequent combination in Caucasians). Alternatively complex effects involving T regulatory cells with these TCR alleles may be involved. Testing of more patients carrying rs1483979C may reveal CAVETDSWGKFQF or other TRAJ24F containing segment(s) with higher $HCRT_{NH2}$ and $pHA_{273-287}$ crossreactivity. Supplementary Table 6 shows examples of possible TRAJ24F associated $HCRT_{NH2}$ sequences, such as TRAV2 CAFTTDSWGKFQF TRAJ24 (10 occurences in a recent onset case) but these occurences were too few to allow any conclusion to be drawn.

An interesting aspect of this data is the strong association of $HCRT_{NH2}$ reactivity to a specific CDR3α segment, TRAV2 CAVETDSWGKLQF TRAJ24, in association with a diversity of CDR3βs. Interestingly, if normally docked, the most conserved N-terminal end portion of $HCRT_{NH2}$ $_{NH2}$-GNHAAGILTL/M$_{-CO-NH2}$ is expected to interact with CDR3α, whereas the more variable amidated C-terminal end should contact CDR3 β possibly contributing to this phenomena. It may be that HCRT amidation induces a broad cross reactivity via CDR3α contacts without as much of a need for tight CDR3β contacts. In this scenario, flu responses, generally more specifically driven by CDR3β contacts[47,56] as most usual epitopes, could occasionally amplify a rare TCR heterodimer containing CDR3β TRBV15 CATSRDTMTSIGTDTQYF, TRBV4−2 CASSQETQGRNYGYTF, TRBV4-3 CASSQGNTGHSPLHF or TRBV4-3 CASSQGDVNYGYTF coupled with TRAV2 CAVETDSWGKLQF TRAJ24 (nodes connecting $pHA_{273-287}$ and $HCRT_{NH2}$

networks in Figure 4b), inducing autoimmunity via cross-reactivity to $HCRT_{NH2}$. Recent analysis of ~80 available TCR-pMHC structures (26 MHC class II) has shown that whereas there is always at least one CDR3β contact with pMHC, there are cases where no CDR3α contact occurs[47,57]. Reverse peptide docking has also been reported in some cases[57] with CDR3β and not CDR3α contacting peptide residues. Similarly, an autoreactive TCR–MHC class II complex found extreme amino-terminal positioning of the TCR over the antigen- binding platform of the MHC molecule, suggesting a link between atypical TCR docking modes and autoreactivity [58], althrough this has not been found in other autoreactive structures. We hypothesise that once a mostly CDR3β driven flu response has TCRα-"hitchhiked" a rare autoreactive clone containing the culprit TRAJ24 CDR3α sequence, $HCRT_{NH2}$ released by damaged hypocretin cells would then amplify a more diverse array of TRAJ24 CDR3α/β response involving other CDR3β with better contacts with $HCRT_{NH2}$ such as TRBV7-2 CASSYDRGSKPQHF, TRBV3-1 CASSQGGTYRETQYF, TRBV20-1 CSASPLGRGTEAFF, TRBV15 CATSSGGGGKAYGYTF, TRBV2 CASSGAGGFYNEQF, TRBV29-1 CSVVSTSASYNEQFF or TRBV9 CASSGTLQGTGGYTF (Supplementary Table 6). Additional studies involving transfection of these heterodimers in TCR reporter-containing TCR deficient Jurkat cell lines, with activation with cognate $pHA_{273-287}$ and $HCRT_{NH2}$ ligands displayed by DQ0602 will be needed to confirm these hypotheses. Cross cultures and structural studies of individual clones would then naturally follow.

A number of molecular mechanisms have been suggested to explain HLA association in autoimmunity[51]. In narcolepsy, major factors likely involve tolerance escape due to PTMs

of the hypocretin autoantigen and crossreactivity with specific flu sequences which may be favored by a primary role of CDR3α in binding this particular autoantigen (a variation of the hotspot binding molecular mimicry hypothesis[51]). Although this study is the first to link specific TCR heterodimers to an autoimmune disease through TCR tetramer sequencing and mendelian randomization, many questions remain un-answered. These include: What is the role of the narcolepsy-associated TRAJ24F allele in disease predisposition? Which flu epitopes besides $pHA_{273-287}$ are involved, notably prior to 2009? What is the role of NP_{17-31}, as minimal or no evidence for mimicry was found with this peptide? What is the role of regulatory T cells and of occasional autoreactivity to non-amidated HCRT or RFX4 fragments? What is the cellular phenotype of the identified autoreactive cells? What portion of normal subjects have crossreactive CDR3α/β-containing T cells in their naïve compartments? Is the presence of TRAV2 CAVETDSWGKLQF TRAJ24 with TRBV4−2 CASSQETQGRNYGYTF in a patient a rare, stochastic occurrence? More extensive tetramer sequencing studies using bar coded tetramers will be needed to fully understand the spectrum of cross reactivity of flu and $HCRT_{NH2}$ autoreactive $CD4^+$ T cells involved in T1N. Most importantly, $HCRT_{NH2}$ autoreactivity appears to be necessary, but not sufficient to induce a full hypocretin neuronal loss and T1N since controls also exhibit some autoreactivity and this remains to be explained. Involvement of regulatory T cells, of other autoantigen(s) and of $CD8^+$ T cells could complete a complex pathophysiological picture, which may serve as a guide to understanding other autoimmune diseases with more complex genetic associations.

Methods

Ethics Statement

This study was reviewed and approved by the Stanford University Institutional Review Board (Protocol # 14325, Registration # 5136). Informed consent was obtained from each participant.

Participants

All patients with narcolepsy (n = 35; 45.7% male; mean age ± standard error of the mean (SEM), 19.0 ± 1.6 years; range, 6 to 53 years) had cataplexy with an onset age of 18.9 ± 1.7 (mean ± SEM) years (ranging from 6 to 53 years) and meet criteria for International Classification of Sleep Disorders 3 (ICSD 3) for type 1 narcolepsy. Cerebrospinal fluid (CSF) hypocretin-1 levels were tested from available 7 patients and all had low level (mean ± SEM, 28.04 ± 13.51 pg/ml, see Supplementary Table 9). 16 out of 35 (45.7%) patients had onset post Pandemrix vaccination, less than one year following vaccination (all in 2009-2010, except for one case vaccinated with Pandemrix in the following season). Controls (n = 22; 59.1% male; mean age ± SEM, 23.3 ± 2.9 years; range, 10 to 57 years) were unrelated subjects, healthy twin or vaccinated siblings. 11 out of 22 (50.0%) controls were vaccinated with Pandemrix. All patients and controls were DQB1*06:02 positive. Peripheral blood mononuclear cells (PBMCs) were collected by apheresis at the Stanford blood center or through phlebotomy, followed by ficoll isolation and storage in liquid nitrogen until use.

Vaccine

The Pandemrix vaccine (A/California/7/2009 (H1N1) NYMC X-179A monovalent bulk (inactivated, sterile)) (Batch# AFLSFDA280) used throughout the study was manufactured with HA content at 139 µg/ml (determined with single radial diffusion (SRD)) by GlaxoSmithKline (GSK) Dresden in January 2010. This batch has been used during the 2009-2010 vaccination campaign in Europe. Summary of Pandemrix characteristics can be found in European medicines agency document (http://www.ema.europa.eu/docs/en_GB/document_library/Other/2010/05/WC500091295.pdf).

Peptides

Overlapping 15-mer peptides (11-amino acid overlap) covering full length of hemagglutinin (HA), neuraminidase (NA), polymerase (basic) protein 1 (PB1), prepro-hyprocretin (HCRT, including post translational modification), 23 variants of nucleoprotein (NP) derived from A/California/07/2009 and A/Puerto Rico/8/1934, and 6 isoforms of regulatory factor X4 (RFX4) (Supplementary Table 1) were synthesized with >90% purity at GenScript NJ and dissolved in dimethyl sulfoxide (DMSO) at a stock concentration of 5 mM or 10 mM as applicable.

Construction of DQ0602

Generation of soluble class II major histocompatibility complex (MHC) was previously described[59]. For DQ0602, truncated coding sequences (CDS) (deletion of signal peptide and transmembrane domain) of human leukocyte antigen (HLA)-DQB1*06:02 (residues

33-230 of NP_002114.3) and HLA-DQA1*01:02 (residues 24-217 of NP_002113.2) were amplified with specific primers (DQB1-F: 5'-TATGGATCCCGGGGCCGGCCCAGTGTCCAAGAT-3', DQB1-R: 5'-TATATGAATTCGCCACCTCTAGACTTGGACTGAGCGCTCTCGC-3'; DQA1-F: 5'-TATGGATCCCGAGGATATCGTCGCCGACCATGTCGC-3', DQA1-R: 5'-TATATGAATTCGCCACCTCTAGACTCTGTGAGTTCGCTCATAG-3') using plasmid DQB1-0602 CLIPmaster (gift from the Emory University NIH tetramer core facility) as a template, respectively. The DQB1 together with class II-associated invariant chain peptide (CLIP) and thrombin cleavage site and DQA1 were then next cloned downstream of a GP67A signal sequence and upstream of a 6*His tag in baculovirus expression vectors 1G4TCRβ and 1G4TCRα[60] (gifts from Garcia lab at Stanford) after double digestion (BamHI/EcoRI), respectively, resulting in 2 chimeric cassettes: CLIP-thrombin cleavage site-DQB1-acidic leucine zipper-biotinylation site-6*His tag and DQA1-basic leucine zipper-6*His tag. As above, HLA-DMA (residues 1-231 of NM_006120.3) and HLA-DMB (residues 1-218 of NM_002118.4) were cloned into plasmids 1G4TCRα and 1G4TCRβ[60] after double digestion (XmaI/EcoRI), respectively. Human cDNA library was used as a template for HLA-DM (DM) with specific primers (DMA-F1: 5'-TCCCCCCGGGATGGGTCATGAACAGAACCAAG-3', DMA-R1: 5'-CCGGAATTCCACATTCTCCAGCAGATCTGAGG-3'; DMB-F1: 5'-TCCCCCCGGGATGATCACATTCCTGCCGC-3', DMB-R1: 5'-CCGGAATTCCTTCAGGGTCTGCATGGGG-3').

Peptide exchange

Purification of monomer class II MHC was previously described[60,61]. Transfection and biotinylation of DQ0602 were conducted using BestBac® 2.0 (Cat# 91-002, Expression Systems) and BirA (Cat# BirA500, Avidity) according to manufacturers' instructions, respectively. Biotinylated DQ0602 (Bio-DQ0602) was isolated by fast protein liquid chromatography (FPLC) at Biomaterials and Advanced Drug Delivery (BioADD) laboratory at Stanford. Peptide exchange[62] was validated with 3 2,4-dinitrophenyl (DNP)-conjugated peptides: Epstein-Barr virus (EBV) nuclear antigen-1 ($EBV_{486-500}$, RALLARSHVERTTDE)[63-65], cytomegalovirus (CMV) phosphoprotein pp65 (CMV_{41-54}, LLQTGIHVRVSQPS)[66], and herpes simplex virus type 2 (HSV-2) VP16 (HSV_{33-50}, PPLYATGRLSQAQLMPSP)[59,67]. Briefly, 5 µg of cleaved Bio-DQ0602 (1 mg/ml) was incubated with 0.25% octyl-β-D-glucoside, 100 mM citrate/NaH_2PO_4 (pH=5.2), 0.4 mg/ml DNP-peptide, and DM (molar ratio of DM:DQ0602=4:1) for 72 h at 37°C, followed by neutralization by adding 1/5 volume of 1 M Tris-HCl (pH=8.0). To analyze peptide exchange efficiency, streptavidin microspheres were added and run on BD LSRII at Stanford Shared FACS Facility (SSFF) after staining with allophycocyanin (APC) anti-HLA-DQ (Cat# 17-9881-42, eBioscience) and anti-DNP (Cat# ab24319, Abcam; isotype, mouse IgE) antibodies, followed by secondary fluorescein isothiocyanate (FITC) anti-mouse IgE (Cat# ab99572, Abcam) antibody.

Generation of peptide-DQ0602 (pDQ0602) tetramer

Generation of class II tetramer was previously described[59,62]. Briefly, the neutralized reaction (above) was incubated with phycoerythrin (PE)-streptavidin (Cat# 405204,

BioLegend) at 6:1 molar ratio of Bio-DQ0602:PE-streptavidin for 1 h at room temperature (RT) in dark. Extra Bio-DQ0602 was removed by streptavidin agarose using a centrifugal filter unit (REF# UFC30GV00, EMD Millipore). pDQ0602 tetramer was concentrated in phosphate buffered saline (PBS, pH=7.4) by centrifugation (REF# UFC510096, EMD Millipore).

Pandemrix cell culture and pDQ0602 tetramer sorting

Tetramer staining was previously described[59,62,68,69]. Briefly, PBMCs were stimulated with100 ng/ml (final concentration of HA) Pandemrix in a 50 ml-culture flask (2.5×10^6 cells/ml) or 6.25 μM peptide in a 96-well plate ($1\text{-}2.5\times10^6$ cells/ml) for 10 or 14 days at 37°C, 5% CO_2. 20 IU/ml IL-2 (Cat# 14-8029-81, eBiosciences) was supplemented from day 7 in complete RPMI medium (RPMI (Cat# 61870-036, Gibco) supplemented with 10% fetal bovine serum (FBS) and 1% penicillin/streptomycin). Medium was changed every 2-4 days. Immediately before staining, pDQ0602 tetramer was spun down to remove aggregates (if any). Fresh or supernatant pDQ0602 tetramer (>10 μg/ml) was incubated with cultured PBMCs in 100 μl of complete RPMI medium for 90 min at 37°C, 5% CO_2. Cells were then stained with a combination of Brilliant Violet 421® (BV421) anti-CD3, Alexa Fluor® 488 (AF488) anti-CD4, Alexa Fluor® 700 (AF700) anti-CD8 and APC/Cy7 anti-CD45RO antibodies (all from BioLegend), followed by analysis on BD LSRII or sorting on BD ARIA II at SSFF. Propidium iodide (PI) was used to gate live cells. Data was analyzed using FlowJo (v10.0.8r1). For most experiments, multiple repeats were done, and if this was the case the mean of repeat observations for each subject was used in statistical analysis.

To complement tetramer data, $CD4^+$ T cells that had been activated by Pandemrix were enriched utilizing an interferon-γ (IFNγ) secretion assay. Briefly, 10-20 million PBMCs were tagged with 0.5 μM carboxyfluorescein diacetate succinimidyl ester (CFSE) (REF# C34554, Life Technologies) in the presence of 100 ng/ml (HA) of Pandemrix and expanded for a 7-day period, whilst supplementing the culture as needed. On day 7, cultured PBMCs were harvested and an aliquot was phenotyped for quantification of T helper subsets as described[70] on BD LSRII. To sort CFSE-low cells, the remaining portion was then stained with a combination of AF647 anti-CD3 (BioLegend), PE/Cy7 anti-CD4 (BioLegend), AF700 anti-CD8 (BD Biosciences) antibodies and the viability dye 7AAD (BioLegend). The CFSE-low $CD4^+$ T cells, which contain the bulk of proliferating cells in response to Pandemrix stimulation, were sorted (minimum of 200,000 cells using a BD ARIA II) into sterile tubes containing advanced RPMI (Cat# 12633-020, Gibco) supplemented with 10 % FBS and 25 mM (4-2-hydroxyethyl)-1-piperazineethanesulfonic acid (HEPES). As a control, an equal number of CFSE-high cells from the CD4 gate, were sorted as described above. The sorted $CD4^+$ T cells were further cultured in high dose IL-2 (500 IU/mL) for 4 days, following which autologous monocytes (CD14 pre-pulsed with 1 μg/mL Pandemrix for 4 h) were added to stimulate sorted CFSE-low versus CFSE-high $CD4^+$ cells in a 1:2 ratio for a 16 h period. Following this, viable IFNγ producing $CD4^+$ T cells were enriched using an IFNγ secretion assay (Miltenyi Biotec) with the two different cell types (CFSE-low & CFSE-high). These were then single cell sorted for T cell receptor (TCR) sequencing (TCRseq) using a BD ARIA II[71]. In subset of individuals (n=2) the pulsing of monocytes with Pandemrix was performed in the presence of 10 μg/mL each

of anti-HLA-DP (REF# H260, Leinco Technologies) and anti-HLA-DQ (Cat# ab23632, Abcam) antibodies.

Competition binding assay

Peptide binding assay was conducted as previously conducted[59,72]. Briefly, 25 nM cleaved DQ0602 was incubated with 100 nM DM, 1 µM biotin-conjugated EBV epitope (Bio-EBV$_{486-500}$, Bio-(GGG)RALLARSHVERTTDE), and 40 µM competitor peptide in reaction buffer (100 mM acetate, pH=4.6, 150 mM NaCl, 1% BSA, 0.5% Nonidet P-40, 0.1% NaN_3) with duplicate for 72 h at 37°C. The reaction was quenched by adding two volumes of neutralization buffer (100 mM Tris-HCl, pH=8.6, 150 mM NaCl, 1% BSA, 0.5 Nonidet P-40, 0.1% NaN_3), followed by incubation with monoclonal anti-DQ (SPV-L3) antibody (Cat# BNUM0200-50, Biotium) (1:400 in 100 mM carbonate-bicarbonate buffer, pH=9.5) in a high binding 96-well plate (REF# 9018, Corning). DELFIA® time-resolved fluorescence (TRF) intensity was detected using a Tecan Infinite® M1000 after successive incubation with 100 µl/well Europium (Eu)-labelled streptavidin (Cat# 1244-360, PerkinElmer) (1:1000, 1% BSA in PBS) and 100 µl/well enhancement solution (Cat# 1244-105, PerkinElmer). Plate was washed 5 times with 300 µl/well wash buffer (0.05% Tween-20 in PBS) to remove nonspecific binding.

Single cell TCR sequencing

Single cell paired TCR sequencing was performed as described[71,73]. Briefly, single cells of $CD3^+CD4^+CD8^-Tetramer^+$ or $IFN\gamma^+CD4^+$ were sorted directly into OneStep® reverse transcription polymerase chain reaction (RT-PCR) buffer (Cat# 210215, Qiagen) in a 96-

well plate, following which the plates were frozen at -80ºC until assayed. Paired TCR CDR3 sequences were obtained by a series of 3 nested PCR reactions. For the first reaction, reverse transcription and pre-amplification were performed with multiplex PCR in a 20 µl of reaction using multiple Vα/Vβ and Cα/Cβ region primers and using the following cycling condition: 50°C 30 min; 95°C 15 min; 94°C 30 s, 62°C 1 min, 72°C 1 min × 25 cycles; 72 °C 5 min; 4 °C 10 min. The second PCR was performed with HotStarTaq® DNA polymerase (Cat# 203205, Qiagen) in a 20 µl of reaction using 1 µl of the first reaction as template and the following cycling condition: 95°C 15 min; 94°C 30 s, 64°C 1 min, 72°C 1 min × 25 cycles (TCR); 72 °C 5 min; 4 °C 10 min. The third PCR incorporated barcodes to enable sequencing on the Illumina® MiSeq platform and was performed in a 20 µl of reaction using 1 µl of the second PCR product as template. Combined PCR products were run on a 1.2% agarose gel. DNA of around 350 to 380 bp was purified and then sequenced on MiSeq platform for a pair-ended 2x250 run. Fastq files were analyzed with a customized TCRseq pipeline at the Human Immune Monitoring Center (HIMC) at Stanford.

TCR Bulk sequencing

TCRα and β repertoires of $CD4^+$ memory T cells isolated from PBMCs were amplified from total ribonucleic acid (RNA) by ARM-PCR procedure as previously described[74] and then sequenced by 2x101 HiSeq 2000 and 2x151 HiSeq 4000 at the Stanford Genome Sequencing Service Center. Data analysis was briefly as follows. The quality of raw fastq files was assessed using FASTQC (http://www.bioinformatics.babraham.ac.uk/projects/fastqc). FLASH was used to merge

the paired end reads[75]. BLAST databases were constructed from IMGT TCRα/β sequences using local blast binaries[76]. The fastq file was converted into fasta and simultaneously processed into equal chunks of fasta records which were then processed using custom python-based analysis pipeline implemented on the Stanford University Genomics Cluster. Each fasta chunk was used to query the BLAST database and identify the TCR C, J & V regions. The CDR3s were then extracted and their frequency along with usage of V, J families computed.

Statistical analyses

Statistical comparisons were performed using two-tailed Mann-Whitney U tests, paired Wilcoxon non parametric tests or Fisher's exact tests whenever most appropriate. Data were plotted using GraphPad PRISM 5. P-value <0.05 were considered statistically significant. All data wrangling and handling was implemented with custom python scripts. R function mantelhaen.test was used to perform Mantel-Haenszel chi-squared test to assess enrichment of TCR families comparing bulk sequencing to single cell sequencing.

For network construction of Figure 4, paired CDR3α/β calls and available alternate CDR3αs for each peptide-specific T cell were pooled in a database. In this database, available CDR3α or CDR3β must pair with one or more corresponding CDR3s across the dataset or are eliminated. Each CDR3α or CDR3β was then used as a key and corresponding CDR3's that pair with the key used as values and matched across the whole dataset using a custom python based pipeline. These matched CDR3αs and CDR3βs was used as template to construct a network object to build a global network of

CDR3α and CDR3β calls across peptides and samples. A python based recursive traversal algorithm was implemented to find local networks i.e. given a CDR3α or CDR3β string, find all the connected CDR3 clusters directly or indirectly to the input CDR3α. This approach was used to extract the TRAJ24 $HCRT_{NH2}$/ $pHA_{273-287}$, NP_{17-31} and $pHA_{273-287}$ local clusters of CDR3s. Node size was calculated based on how many connections a particular CDR3 accepts or sends out, while the edge or connected line thickness was based on total counts of that particular CDR3α/β pair.

Legends to Figures

Figure 1: Results of primary tetramer screening in 10 subjects: a. Tetramer positivity in post-Pandemrix® patients (dark grey, from 5 total), post-Pandemrix® controls (light grey, from 4 total) and one early onset patient (onset=0.3 year prior, blue, single subject). Tetramers were built one by one using peptide exchange using a DQ0602-CLIP (see Methods). *Viral protein tetramers:* HA=Hemagglutinin, NA= Neuraminidase, NP= Nucleoproteins, PB1= Polymerase Basic 1. Binder sequences from influenza A/reassortant/NYMC X-179A (reference ADE2909) were primarily used. X179A is a reassortant of A/California/07/2009 (pandemic pH1N1 2009) with A/Puerto Rico/8/1934. A/Puerto Rico/8/1934, is an old pre-2009 H1N1 strain, commonly called PR8, representative of seasonal H1N1 strains prior to the 2009-2010 pandemic and still circulating at low levels. In X-179A the primary sequence of HA, NA and PB1 is from pH1N1 while the NP sequence is from PR8. Any polymorphic peptide sequence differing in NP (A/California/07/2009) between PR8 (/Puerto Rico/8/and pH1N1) that still bound to DQ0602 was also tested and is labelled with a star (others are of PR8 origin). s=epitope

of identical sequence in PR8 and pH1N1. Subjects were tested with tetramers after culture with Pandemrix 100 ng/ml for 10 days. *Autoantigen tetramers:* HCRT= prepro-hypocretin, RFX4=all known isoforms of Regulatory Factor X4, last six peptides=post-translationally modified sequences of prepro-HCRT modified as per secreted hypocretin-1 and 2, when binding DQ0602, including N-Pyroglutamate $HCRT_{34-48}$ plus $HCRT_{38-52}$, $HCRT_{33-47}$ and $HCRT_{37-51}$ with two double disulfide bonds (DB), C-terminal amidated $HCRT_{54-66}$ and $HCRT_{86-97}$ denoted $HCRT_{54-66-NH2}$ and $HCRT_{86-97-NH2}$, as in secreted, mature hypocretin-1 and 2. Subjects were tested after a 10-day culture with 6.25 µM of each peptide. The main epitopes selected for further analysis are labelled above each bar (based on immunodominance and likely difference between narcolepsy and controls). Peptides $pHA_{209-223}$, $pHA_{273-287}$, $pHA_{321-335}$, $pHA_{437-451}$, pNA_{45-59}, $pNA_{217-231}$, $pNA_{217-231}$, NP_{17-31}, $NP_{261-275s}$ (shared epitope between pH1N1 and PR8), and $NP_{437-451-pH1N1}$* are responding in 60% of subjects and are considered immunodominants in the DQ0602 response to H1N1. $NP_{17-31-pH1N1}$ the sequence equivalent to NP_{17-31} but derived from pH1N1 instead of backbone PR8 sequence. HA69 ($pHA_{273-287}$) does not have a strong binder in the same area for PR8. b. Distribution of positive subjects per antigen. Note that response to HA, NA and NP, the main antigens contained in Pandemrix® and known to be responsive to flu infections have the large number of positive subjects (≥ 2) whereas binders from autoantigens RFX4 and HCRT only show sporadic response in a maximum of 2 subjects. c. Mean percent of subjects positive for DQ0602 binders in each proteins in post Pandemrix® subjects. Note that viral peptides derived from HA, NA and NP peptides have a large number of responders (36±3%, n=55) in comparison to lower abundance protein PB1 (26±5%, n=7). The response of non-modified autoantigen

sequence is lowest at 5±1%. (n=67). In contrast, the response to post translationally modified (PTM)-modified hypocretin fragment is high (40± 16%, n=6), approaching that of foreign, viral antigens (see t-test statistics in figure). d. Example of FACS staining obtained for various selected tetramers. The entire dataset of FACS staining plots is provided as Extended Data Figure 1. Note tail-like staining in many (but not all) cases with $HCRT_{86\text{-}97\text{-}NH2}$ but not with other tetramers.

Figure 2: Results of secondary tetramer screening using $pHA_{273\text{-}287}$, $NP_{17\text{-}31}$, $HCRT_{54\text{-}66}$, $HCRT_{54\text{-}66\text{-}NH2}$, $HCRT_{86\text{-}97}$, and $HCRT_{86\text{-}97\text{-}NH2}$ in 35 patients and 22 controls. Tetramers were built one by one using peptide exchange using a DQ0602-CLIP (see Methods). a. Percent of subjects with $pHA_{273\text{-}287}$ and $NP_{17\text{-}31}$ tetramer positivity in controls versus patients. PBMCs of subjects were grown in Pandemrix® or the cognate peptide for 10 days in two independent experiments, and as results were repeatable and did not differ statistically, the mean is presented in each dot. T, twins. Subjects in red are those with single cell sorting and sequencing data available. Number of subjects tested is under parenthesis. b. Percent of subjects with $HCRT_{54\text{-}66}$/$HCRT_{54\text{-}66\text{-}NH2}$ and $HCRT_{86\text{-}97}$ /$HCRT_{86\text{-}97\text{-}NH2}$ tetramer positivity in controls versus patients. PBMCs of subjects were grown with the cognate peptide for 10 or 14 days in two independent experiments, and as results were repeatable and did not differ statistically, the mean is presented in each dot. T, twins. Subjects in red are those with single cell sorting and sequencing data available. c: Example of $pHA_{273\text{-}287}$ and $NP_{17\text{-}31}$ tetramer staining in a few subjects (for all results, see Extended Data Figure 1). d. Example of $HCRT_{54\text{-}66}$, $HCRT_{54\text{-}66\text{-}NH2}$, $HCRT_{86\text{-}97}$, and $HCRT_{86\text{-}97\text{-}NH2}$ tetramer staining in a few subjects (for all results, see Extended Data

Figure 1). Note the "tail-like staining" aspect of $HCRT_{86-97-NH2}$ often found with this peptide, although occasional distinct monoclonal population can be observed.

Figure 3: Shared CDR3α, CDR3β and CDR3α/β sequences for $pHA_{273-287}$ (a), NP_{17-31}, (b), $HCRT_{54-66-NH2}$ (c), and $HCRT_{86-97-NH2}$ (d), across subjects. Red: number of patients with corresponding CDR3, Grey, number of controls with same CDR3 (per horizontal axis). Box numbers indicate total of times when the CDR3 occurred across patients and controls. e: $pHA_{273-287}$, NP_{17-31}, $HCRT_{54-66-NH2}$, and $HCRT_{86-97-NH2}$ sequence homology assessed using http://tools.iedb.org/cluster/reference/[46] with three EBV sequences used as anchor. Note high similarity of $HCRT_{54-66-NH2}$, and $HCRT_{86-97-NH2}$, also share homology with $pHA_{273-287}$[18,24] as previously reported, but not NP_{17-31}. Note extensive sharing of TRAJ24 (labelled in red) CDR3 CAVETDSWGKLQF in patients and controls with $HCRT_{54-66-NH2}$ and $HCRT_{86-97-NH2}$. In most cases, these CRD3α CAVETDSWGKLQF do not share the same CDR3β (see Supplementary Table 4). We also found sharing of TRBV4-2 containing CRD3β CASSQERGSYNEQFF (labelled in red) in patients with NP_{17-31} only and sharing of TRBV4-2 containing CRD3β CASSQETQGRNYGYTF (labelled in red) in $pHA_{273-287}$ and $HCRT_{NH2}$ associated tetramers although these do not share a similar CRD3α (see supplementary Table 4).

Figure 4: . Network clustering of TCR segments obtained through tetramer sequencing: (a) global view of the generated network with its 3 central clusters; (b) $pHA_{273-287}$/ $HCRT_{NH2}$ cluster centered around TRAJ24; (c) $pHA_{273-287}$ specific cluster ; and (d) NP_{17-31} specific cluster. Tree formation was computed using a partional recursive clustering

elimination algorithm implemented using Python. Each node represents a CDR3α or a CDR3β segment, with size proportional to occurrences. Lines connecting these clusters represent heterodimers, with thickness proportional to clone number. Color coding corresponds to type of tetramer ($pHA_{273-287}$, $HCRT_{NH2}$ or NP_{17-31}) yielding specific clones. Note that Cluster (b), primarily derived from $HCRT_{NH2}$ tetramers and centered around CDR3α TRAV2_CAVETDSWGKLQF_TRAJ24, is hybrid, containing not only CDR3β recruited by $HCRT_{NH2}$ but also CDR3β chains more frequently recruited by $pHA_{273-287}$ and occasionally recruited by $HCRT_{NH2}$ TRBV4-2_CASSQETQGRNYGYTF (141), TRBV15_CATSRDTMTSIGTDTQYF (105), TRBV4-3_CASSQGNTGHSPLHF (96) and TRBV4-3_CASSQGDVNYGYTF (10) (see supplementary Table 5 and 6). One small direct connection between TRAV2_CAVETDSWGKLQF_TRAJ24 and TRBV20-1_CSASPLGRGTEAF (17) primarily used by NP_{17-31} is also present, suggesting that some limited mimicry may also occur with NP_{17-31}. Abundantly expressed TRAV26-1_CIVRSQGGSYIPTF_TRAJ6 is a CDR3α and is indirectly linked. Note also NP_{17-31}-CDR3α TRAV13-2_CAENPNNAGNMLTF_AJ39 (64), a possible link to NP_{17-31} but through a CDR3α; as CDR3α are more likely to be shared by chance and this is peripheral to the network, significance is uncertain.

Acknowledgments

The study was funded by gifts from Wake Up Narcolepsy, Jazz Pharmaceutical and individual patients to Stanford University. Some samples have been gathered by defunct NIH grant P50-NS-23724 to Emmanuel Mignot (ended in 2016). Bulk Sequencing and some sample collection has been funded by a prior grant from Glaxo Smith Kline (GSK),

supervised by the European Medical Agency (ended in 2014), with corresponding data reported in Ollila et al.[29]. Note that none of the current authors have been involved in the generation of fraudulent ELISpot results reported in the retracted De la Herran-Arita et al. publication[18,24], as determined by a review of Stanford's internal investigation report by NIH Office of Research Integrity. Dr. Mignot occasionally consults and has received contracts from Jazz Pharmaceuticals and is and has been a Principal Investigator on clinical trials using sodium oxybate and Solriamfetol, Jazz Pharmaceutical products, in the treatment of narcolepsy; none of these have any scientific relationship to the study. This work used the Genome Sequencing Service Center by Stanford Center for Genomics and Personalized Medicine Sequencing Center, supported by the grant award NIH S10OD020141. We thank Dr. K. Christopher Garcia for sharing plasmids and insect cell lines and NIH tetramer core facility for sharing DQA1*01:02/DQB1*0602 expression construct. We thank Wenchao Sun from Stanford Biomaterials and Advanced Drug Delivery Lab (BioADD) for HPLC running and Stanford FACS facility for providing analyzers and sorters and technical support.

Supporting information

Supplementary Table 1. Screening of HA, NA, NP, PB1, HCRT and RFX4 overlapping peptides for DQ0602 binding.

Supplementary Table 2. DQ0602 registers of main peptides and sequences used for confirmatory tetramer studies.

Supplementary Table 3. Single cell sequencing TCR segment usage preference in cases and controls.

Supplementary Table 4. Sharing of CDR3α, CDR3β and CDR3αβ pairs across epitopes/individuals.

Supplementary Table 5. Significant CDR3 motifs across peptides and individual.

Supplementary Table 6. TRAJ24 positive clones found in patients and controls with various antigens.

Supplementary Table 7. TRBV4-2 positive clones found in patients and controls with various antigens.

Supplementary Table 8. TCR sharing of tetramer with IFNγ positive cells cultured with Pandemrix.

Supplementary Table 9. Clinical characteristics and use of subjects in this study.

References

1 Han, F. *et al.* Genome wide analysis of narcolepsy in China implicates novel immune loci and reveals changes in association prior to versus after the 2009 H1N1 influenza pandemic. *PLoS Genet* **9**, e1003880, doi:10.1371/journal.pgen.1003880 (2013).

2 Faraco, J. *et al.* ImmunoChip study implicates antigen presentation to T cells in narcolepsy. *PLoS Genet* **9**, e1003270, doi:10.1371/journal.pgen.1003270 (2013).

3 Kornum, B. R. *et al.* Common variants in P2RY11 are associated with narcolepsy. *Nat Genet* **43**, 66-71, doi:10.1038/ng.734 (2011).

4 Hor, H. *et al.* Genome-wide association study identifies new HLA class II haplotypes strongly protective against narcolepsy. *Nat Genet* **42**, 786-789, doi:10.1038/ng.647 (2010).

5 Hallmayer, J. *et al.* Narcolepsy is strongly associated with the T-cell receptor alpha locus. *Nat Genet* **41**, 708-711, doi:10.1038/ng.372 (2009).

6 Ollila, H. M. *et al.* HLA-DPB1 and HLA class I confer risk of and protection from narcolepsy. *Am J Hum Genet* **96**, 136-146, doi:10.1016/j.ajhg.2014.12.010 (2015).

7 Martinez-Orozco, F. J., Vicario, J. L., De Andres, C., Fernandez-Arquero, M. & Peraita-Adrados, R. Comorbidity of Narcolepsy Type 1 With Autoimmune Diseases and Other Immunopathological Disorders: A Case-Control Study. *J Clin Med Res* **8**, 495-505, doi:10.14740/jocmr2569w (2016).

8 Singh, A. K., Mahlios, J. & Mignot, E. Genetic association, seasonal infections and autoimmune basis of narcolepsy. *J Autoimmun* **43**, 26-31, doi:10.1016/j.jaut.2013.02.003 (2013).

9 Aran, A. *et al.* Elevated anti-streptococcal antibodies in patients with recent narcolepsy onset. *Sleep* **32**, 979-983 (2009).

10 Han, F. *et al.* Narcolepsy onset is seasonal and increased following the 2009 H1N1 pandemic in China. *Ann Neurol* **70**, 410-417, doi:10.1002/ana.22587 (2011).

11 Dye, T. J., Gurbani, N. & Simakajornboon, N. Epidemiology and Pathophysiology of Childhood Narcolepsy. *Paediatr Respir Rev* **25**, 14-18, doi:10.1016/j.prrv.2016.12.005 (2018).

12 Feltelius, N. *et al.* A coordinated cross-disciplinary research initiative to address an increased incidence of narcolepsy following the 2009-2010 Pandemrix vaccination programme in Sweden. *J Intern Med* **278**, 335-353, doi:10.1111/joim.12391 (2015).

13 Ambati, A. *et al.* Increased beta-haemolytic group A streptococcal M6 serotype and streptodornase B-specific cellular immune responses in Swedish narcolepsy cases. *J Intern Med* **278**, 264-276, doi:10.1111/joim.12355 (2015).

14 Vaarala, O. *et al.* Antigenic differences between AS03 adjuvanted influenza A (H1N1) pandemic vaccines: implications for pandemrix-associated narcolepsy risk. *PLoS One* **9**, e114361, doi:10.1371/journal.pone.0114361 (2014).

15 Nishino, S., Ripley, B., Overeem, S., Lammers, G. J. & Mignot, E. Hypocretin (orexin) deficiency in human narcolepsy. *Lancet* **355**, 39-40, doi:10.1016/s0140-6736(99)05582-8 (2000).

16 Peyron, C. *et al.* A mutation in a case of early onset narcolepsy and a generalized absence of hypocretin peptides in human narcoleptic brains. *Nat Med* **6**, 991-997, doi:10.1038/79690 (2000).

17 Thannickal, T. C. *et al.* Reduced number of hypocretin neurons in human narcolepsy. *Neuron* **27**, 469-474 (2000).

18 De la Herran-Arita, A. K. *et al.* CD4+ T cell autoimmunity to hypocretin/orexin and cross-reactivity to a 2009 H1N1 influenza A epitope in narcolepsy. *Sci Transl Med* **5**, 216ra176, doi:10.1126/scitranslmed.3007762 (2013).

19 Kornum, B. R. *et al.* Absence of autoreactive CD4(+) T-cells targeting HLA-DQA1*01:02/DQB1*06:02 restricted hypocretin/orexin epitopes in narcolepsy type 1 when detected by EliSpot. *J Neuroimmunol* **309**, 7-11, doi:10.1016/j.jneuroim.2017.05.001 (2017).

20 Ramberger, M. *et al.* CD4+ T-Cell Reactivity to Orexin/Hypocretin in Patients With Narcolepsy Type 1. *Sleep* **40**, doi:10.1093/sleep/zsw070 (2017).

21 Tanaka, S., Honda, Y., Inoue, Y. & Honda, M. Detection of autoantibodies against hypocretin, hcrtrl, and hcrtr2 in narcolepsy: anti-Hcrt system antibody in narcolepsy. *Sleep* **29**, 633-638 (2006).

22 Ahmed, S. S. *et al.* Antibodies to influenza nucleoprotein cross-react with human hypocretin receptor 2. *Sci Transl Med* **7**, 294ra105, doi:10.1126/scitranslmed.aab2354 (2015).

23 Cvetkovic-Lopes, V. *et al.* Elevated Tribbles homolog 2-specific antibody levels in narcolepsy patients. *J Clin Invest* **120**, 713-719, doi:10.1172/jci41366 (2010).

24 De la Herran-Arita, A. K. *et al.* Retraction of the research article: "CD4(+) T cell autoimmunity to hypocretin/orexin and cross-reactivity to a 2009 H1N1 influenza A epitope in narcolepsy". *Sci Transl Med* **6**, 247rt241, doi:10.1126/scitranslmed.3009995 (2014).

25 Giannoccaro, M. P. *et al.* Antibodies Against Hypocretin Receptor 2 Are Rare in Narcolepsy. *Sleep* **40**, doi:10.1093/sleep/zsw056 (2017).

26 Luo, G. *et al.* Absence of anti-hypocretin receptor 2 autoantibodies in post pandemrix narcolepsy cases. *PLoS One* **12**, e0187305, doi:10.1371/journal.pone.0187305 (2017).

27 Lind, A. *et al.* A/H1N1 antibodies and TRIB2 autoantibodies in narcolepsy patients diagnosed in conjunction with the Pandemrix vaccination campaign in Sweden 2009-2010. *J Autoimmun* **50**, 99-106, doi:10.1016/j.jaut.2014.01.031 (2014).

28 van der Heide, A., Hegeman-Kleinn, I. M., Peeters, E., Lammers, G. J. & Fronczek, R. Immunohistochemical screening for antibodies in recent onset type 1 narcolepsy and after H1N1 vaccination. *J Neuroimmunol* **283**, 58-62, doi:10.1016/j.jneuroim.2015.04.008 (2015).

29 Ollila, H. *et al.* Narcolepsy risk loci are enriched in immune cells and suggest autoimmune modulation of the T cell receptor repertoire. *bioRxiv* (2018).

30 Bernard-Valnet, R. *et al.* CD8 T cell-mediated killing of orexinergic neurons induces a narcolepsy-like phenotype in mice. *Proc Natl Acad Sci U S A* **113**, 10956-10961, doi:10.1073/pnas.1603325113 (2016).

31 Longstreth, W. T., Jr., Ton, T. G. & Koepsell, T. D. Narcolepsy and streptococcal infections. *Sleep* **32**, 1548 (2009).

32 Han, F., Lin, L., Li, J., Dong, X. S. & Mignot, E. Decreased incidence of childhood narcolepsy 2 years after the 2009 H1N1 winter flu pandemic. *Ann Neurol* **73**, 560, doi:10.1002/ana.23799 (2013).

33 Wu, H. *et al.* Symptoms and occurrences of narcolepsy: a retrospective study of 162 patients during a 10-year period in eastern China. *Sleep Med* **15**, 607-613, doi:10.1016/j.sleep.2013.12.012 (2014).

34 Gomez-Bautista, M., Rojo-Vazquez, F. A. & Alunda, J. M. The effect of the host's age on the pathology of Eimeria stiedai infection in rabbits. *Vet Parasitol* **24**, 47-57 (1987).

35 Jacob, L. *et al.* Comparison of Pandemrix and Arepanrix, two pH1N1 AS03-adjuvanted vaccines differentially associated with narcolepsy development. *Brain Behav Immun* **47**, 44-57, doi:10.1016/j.bbi.2014.11.004 (2015).

36 Ollila, H. M., Fernandez-Vina, M. & Mignot, E. HLA-DQ allele competition in narcolepsy: a comment on Tafti et al. DQB1 locus alone explains most of the risk and protection in narcolepsy with cataplexy in Europe. *Sleep* **38**, 147-151, doi:10.5665/sleep.4342 (2015).

37 Han, F. *et al.* HLA-DQ association and allele competition in Chinese narcolepsy. *Tissue Antigens* **80**, 328-335, doi:10.1111/j.1399-0039.2012.01948.x (2012).

38 Miyagawa, T. *et al.* New susceptibility variants to narcolepsy identified in HLA class II region. *Hum Mol Genet* **24**, 891-898, doi:10.1093/hmg/ddu480 (2015).

39 Mignot, E. *et al.* Complex HLA-DR and -DQ interactions confer risk of narcolepsy-cataplexy in three ethnic groups. *Am J Hum Genet* **68**, 686-699 (2001).

40 Tafti, M. *et al.* DQB1 locus alone explains most of the risk and protection in narcolepsy with cataplexy in Europe. *Sleep* **37**, 19-25, doi:10.5665/sleep.3300 (2014).

41 Bedford, T., Cobey, S., Beerli, P. & Pascual, M. Global migration dynamics underlie evolution and persistence of human influenza A (H3N2). *PLoS Pathog* **6**, e1000918, doi:10.1371/journal.ppat.1000918 (2010).

42 Nicolson, C. *et al.* An additional oligosaccharide moiety in the HA of a pandemic influenza H1N1 candidate vaccine virus confers increased antigen yield in eggs. *Vaccine* **30**, 745-751, doi:10.1016/j.vaccine.2011.11.081 (2012).

43 Demachi-Okamura, A. *et al.* Epstein-Barr virus nuclear antigen 1-specific CD4+ T cells directly kill Epstein-Barr virus-carrying natural killer and T cells. *Cancer Sci* **99**, 1633-1642, doi:10.1111/j.1349-7006.2008.00852.x (2008).

44 Dalal, J. *et al.* Translational profiling of hypocretin neurons identifies candidate molecules for sleep regulation. *Genes Dev* **27**, 565-578, doi:10.1101/gad.207654.112 (2013).

45 Sharon, E. *et al.* Genetic variation in MHC proteins is associated with T cell receptor expression biases. *Nat Genet* **48**, 995-1002, doi:10.1038/ng.3625 (2016).

46 Kim, Y. *et al.* Immune epitope database analysis resource. *Nucleic Acids Res* **40**, W525-530, doi:10.1093/nar/gks438 (2012).

47 Glanville, J. *et al.* Identifying specificity groups in the T cell receptor repertoire. *Nature* **547**, 94-98, doi:10.1038/nature22976 (2017).

48 Xu, P. *et al.* Conditional ablation of the RFX4 isoform 1 transcription factor: Allele dosage effects on brain phenotype. *PLoS One* **13**, e0190561, doi:10.1371/journal.pone.0190561 (2018).

49 Dauvilliers, Y. *et al.* Hypothalamic immunopathology in anti-Ma-associated diencephalitis with narcolepsy-cataplexy. *JAMA Neurol* **70**, 1305-1310, doi:10.1001/jamaneurol.2013.2831 (2013).

50 Sakurai, T. *et al.* Orexins and orexin receptors: a family of hypothalamic neuropeptides and G protein-coupled receptors that regulate feeding behavior. *Cell* **92**, 573-585 (1998).

51 Dendrou, C. A., Petersen, J., Rossjohn, J. & Fugger, L. HLA variation and disease. *Nat Rev Immunol* **18**, 325-339, doi:10.1038/nri.2017.143 (2018).

52 Raposo, B. *et al.* T cells specific for post-translational modifications escape intrathymic tolerance induction. *Nat Commun* **9**, 353, doi:10.1038/s41467-017-02763-y (2018).

53 Risnes, L. F. *et al.* Disease-driving CD4+ T cell clonotypes persist for decades in celiac disease. *J Clin Invest* **128**, 2642-2650, doi:10.1172/JCI98819 (2018).

54 Cushing, A. *et al.* Emergence of Hemagglutinin Mutations During the Course of Influenza Infection. *Sci Rep* **5**, 16178, doi:10.1038/srep16178 (2015).

55 Montplaisir, J. *et al.* Risk of narcolepsy associated with inactivated adjuvanted (AS03) A/H1N1 (2009) pandemic influenza vaccine in Quebec. *PLoS One* **9**, e108489, doi:10.1371/journal.pone.0108489 (2014).

56 Song, I. *et al.* Broad TCR repertoire and diverse structural solutions for recognition of an immunodominant CD8(+) T cell epitope. *Nat Struct Mol Biol* **24**, 395-406, doi:10.1038/nsmb.3383 (2017).

57 La Gruta, N. L., Gras, S., Daley, S. R., Thomas, P. G. & Rossjohn, J. Understanding the drivers of MHC restriction of T cell receptors. *Nat Rev Immunol* **18**, 467-478, doi:10.1038/s41577-018-0007-5 (2018).

58 Hahn, M., Nicholson, M. J., Pyrdol, J. & Wucherpfennig, K. W. Unconventional topology of self peptide-major histocompatibility complex binding by a human autoimmune T cell receptor. *Nat Immunol* **6**, 490-496, doi:10.1038/ni1187 (2005).

59 Kwok, W. W. *et al.* HLA-DQ Tetramers Identify Epitope-Specific T Cells in Peripheral Blood of Herpes Simplex Virus Type 2-Infected Individuals: Direct Detection of Immunodominant Antigen-Responsive Cells. *The Journal of Immunology* **164**, 4244-4249, doi:10.4049/jimmunol.164.8.4244 (2000).

60 Birnbaum, M. E. *et al.* Molecular architecture of the αβ T cell receptor–CD3 complex. *Proceedings of the National Academy of Sciences* **111**, 17576-17581, doi:10.1073/pnas.1420936111 (2014).

61 Qi, Q. *et al.* Defective T Memory Cell Differentiation after Varicella Zoster Vaccination in Older Individuals. *PLOS Pathogens* **12**, e1005892, doi:10.1371/journal.ppat.1005892 (2016).

62 Day, C. L. *et al.* Ex vivo analysis of human memory CD4 T cells specific for hepatitis C virus using MHC class II tetramers. *Journal of Clinical Investigation* **112**, 831-842, doi:10.1172/JCI200318509 (2003).

63 Demachi-Okamura, A. *et al.* Epstein–Barr virus nuclear antigen 1-specific CD4+ T cells directly kill Epstein–Barr virus-carrying natural killer and T cells. *Cancer Science* **99**, 1633-1642, doi:10.1111/j.1349-7006.2008.00852.x (2008).

64 Leen, A. *et al.* Differential Immunogenicity of Epstein-Barr Virus Latent-Cycle Proteins for Human CD4(+) T-Helper 1 Responses. *Journal of Virology* **75**, 8649-8659, doi:10.1128/JVI.75.18.8649-8659.2001 (2001).

65 Bickham, K. *et al.* EBNA1-specific CD4(+) T cells in healthy carriers of Epstein-Barr virus are primarily Th1 in function. *Journal of Clinical Investigation* **107**, 121-130 (2001).

66 Gallot, G. *et al.* Purification of Ag-Specific T Lymphocytes After Direct Peripheral Blood Mononuclear Cell Stimulation Followed by CD25 Selection. I. Application to CD4⁺ or CD8⁺ Cytomegalovirus Phosphoprotein pp65 Epitope Determination. *The Journal of Immunology* **167**, 4196-4206, doi:10.4049/jimmunol.167.8.4196 (2001).

67 Reichstetter, S. *et al.* Cytotoxic herpes simplex type 2-specific, DQ0602-restricted CD4(+) T-cell clones show alloreactivity to DQ0601. *Immunology* **117**, 350-357, doi:10.1111/j.1365-2567.2005.02308.x (2006).

68 Newell, E. W., Klein, L. O., Yu, W. & Davis, M. M. Simultaneous detection of many T-cell specificities using combinatorial tetramer staining. *Nature methods* **6**, 497-499, doi:10.1038/nmeth.1344 (2009).

69 Reijonen, H. & Kwok, W. W. Use of HLA class II tetramers in tracking antigen-specific T cells and mapping T-cell epitopes. *Methods* **29**, 282-288, doi:https://doi.org/10.1016/S1046-2023(02)00350-X (2003).

70 Becattini, S. *et al.* Functional heterogeneity of human memory CD4⁺ T cell clones primed by pathogens or vaccines. *Science* **347**, 400 (2015).

71 Han, A., Glanville, J., Hansmann, L. & Davis, M. M. Linking T-cell receptor sequence to functional phenotype at the single-cell level. *Nature biotechnology* **32**, 684-692, doi:10.1038/nbt.2938 (2014).

72 Ettinger, R. A. & Kwok, W. W. A Peptide Binding Motif for HLA-DQA1*0102/DQB1*0602, the Class II MHC Molecule Associated with Dominant Protection in Insulin-Dependent Diabetes Mellitus. *The Journal of Immunology* **160**, 2365 (1998).

73 Glanville, J. *et al.* Identifying specificity groups in the T cell receptor repertoire. *Nature* **547**, 94-98, doi:10.1038/nature22976 (2017).

74 Wang, C. *et al.* High throughput sequencing reveals a complex pattern of dynamic interrelationships among human T cell subsets. *Proceedings of the National Academy of Sciences of the United States of America* **107**, 1518-1523, doi:10.1073/pnas.0913939107 (2010).

75 Magoc, T. & Salzberg, S. L. FLASH: fast length adjustment of short reads to improve genome assemblies. *Bioinformatics* **27**, 2957-2963, doi:10.1093/bioinformatics/btr507 (2011).

76 Altschul, S. F., Gish, W., Miller, W., Myers, E. W. & Lipman, D. J. Basic local alignment search tool. *Journal of Molecular Biology* **215**, 403-410, doi:https://doi.org/10.1016/S0022-2836(05)80360-2 (1990).

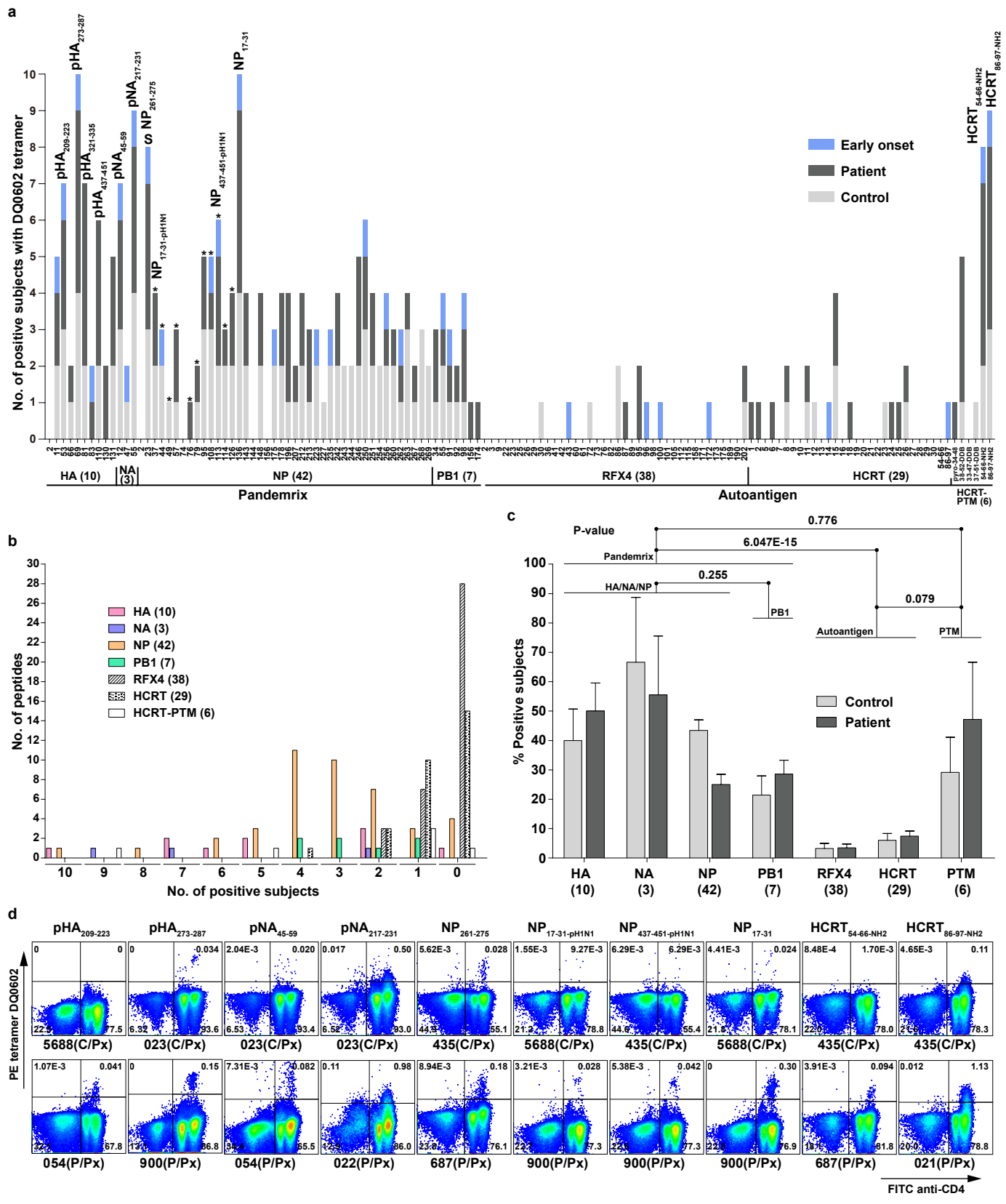

Figure 1 | Results of primary tetramer screening in 10 subjects. **a**. Tetramer positivity in 5 post Pandemrix patients (P/Px), 4 post Pandemrix controls (C/Px) and one early onset patient (onset=0.3 year). Immunodominant epitopes are indicated. Number of peptides for each antigen is shown between brackets. PTM, post translational modification. S, shared by A/California/07/2009 and A/Puerto Rico/8/1934. * deriving from A/California/07/2009. For peptide and subject infomation, see Supplementary Table 1 and 9, respectively. **b**. Distribution of positive subjects per antigen. **c**. Mean percentage of subjects positive for DQ0602 tetramers in each antigen in patients and controls. Statistics between groups of antigens were calculated. **d**. Example of FACS staining obtained for various selected tetramers. $CD3^+$ T cells are shown with frequency. The entire dataset of FACS staining plots is provided as Extended Data Figure 1. Note tail-like staining in many (but not all) cases with $HCRT_{86\text{-}97\text{-}NH2}$ but not with other tetramers.

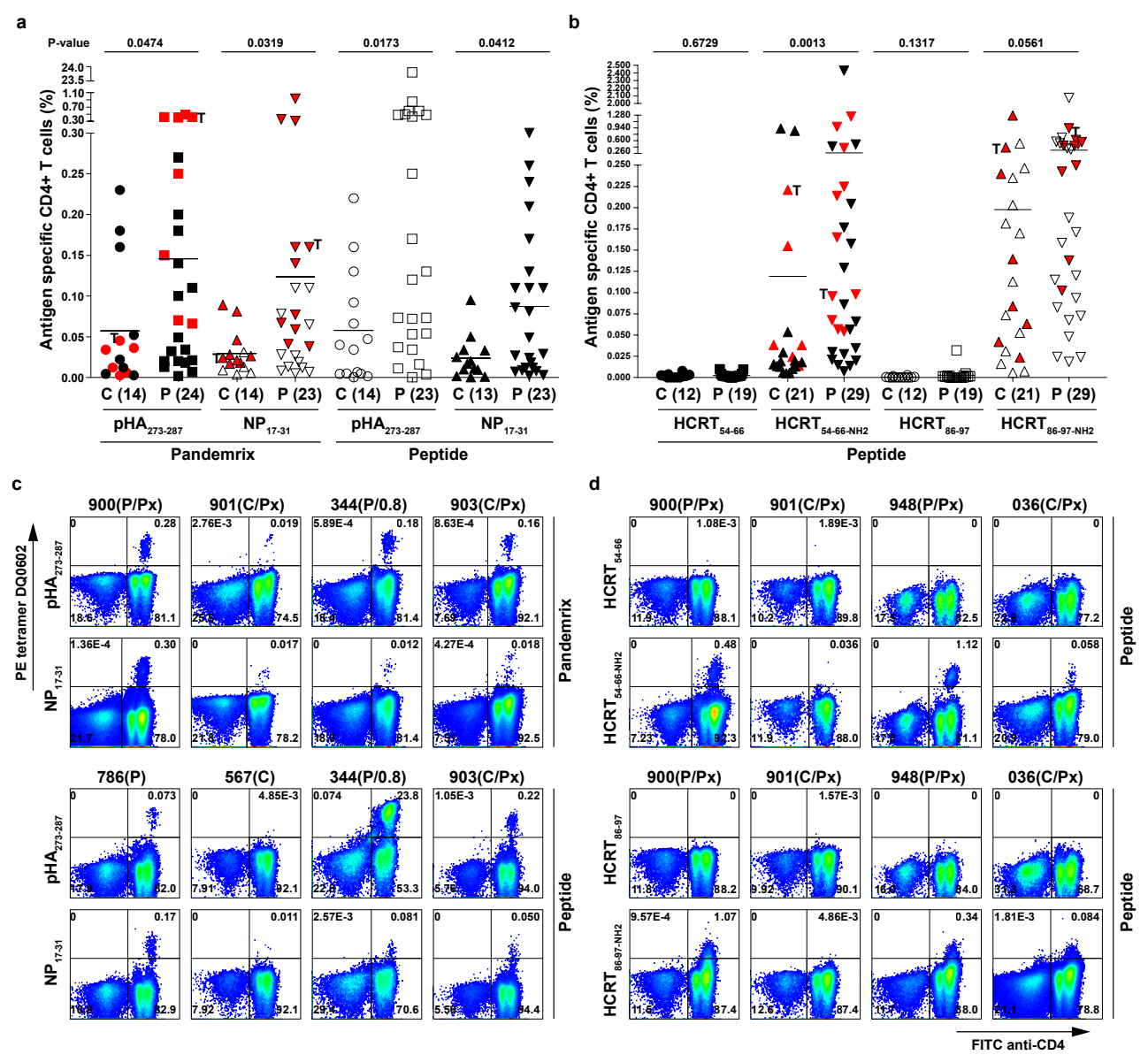

Figure 2 | Results of secondary tetramer screening using $pHA_{273-287}$, NP_{17-31}, $HCRT_{54-66}$, $HCRT_{54-66-NH2}$, $HCRT_{86-97}$, and $HCRT_{86-97-NH2}$. **a**. Tetramer positivity of $pHA_{273-287}$ and NP_{17-31} in controls versus patients stimulated with Pandemrix or peptide. **b**. Tetramer positivity of $HCRT_{54-66}$/$HCRT_{54-66-NH2}$ and $HCRT_{86-97}$/$HCRT_{86-97-NH2}$ in controls versus patients stimulated with peptide. **c**. Example of $pHA_{273-287}$ and NP_{17-31} staining in a few subjects. **d**. Example of $HCRT_{54-66}$, $HCRT_{54-66-NH2}$, $HCRT_{86-97}$, and $HCRT_{86-97-NH2}$ tetramer staining in a few subjects (for all results, see Extended Data Figure 1). P, patient; P/Px, post Pandemrix patient; C, control; C/Px, post Pandemrix control. Interval is shown if patient is early onset (<1.0 year); T, twins; Red, single cell TCR sequencing. $CD3^+$ T cells are shown in c and d with frequency.

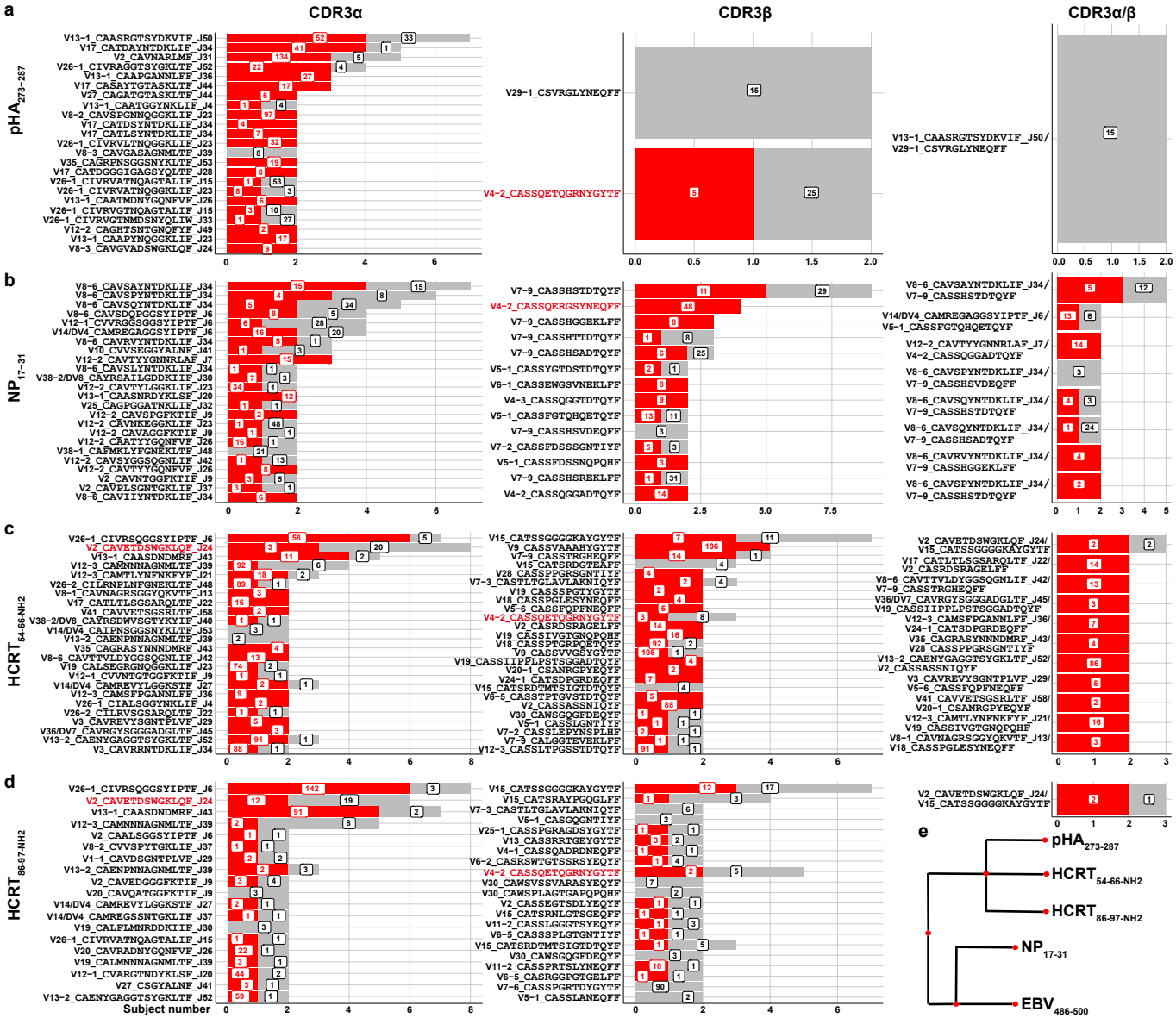

Figure 3 | Shared CDR3α, CDR3β and CDR3α/β sequences for $pHA_{273-287}$ (a), NP_{17-31} (b), $HCRT_{54-66-NH2}$ (c) and $HCRT_{86-97-NH2}$ (d) across subjects. Red, number of patients with corresponding CDR3 (per horizontal axis); Grey, number of controls with same CDR3 (per horizontal axis). Box numbers indicate total of times when the CDR3 occurred across patients and controls. **e**. $pHA_{273-287}$, NP_{17-31}, $HCRT_{54-66-NH2}$ and $HCRT_{86-97-NH2}$ sequence homology with $EBV_{486-500}$ used as anchor. TRAJ24 and TRBV4-2 are labeled in red.

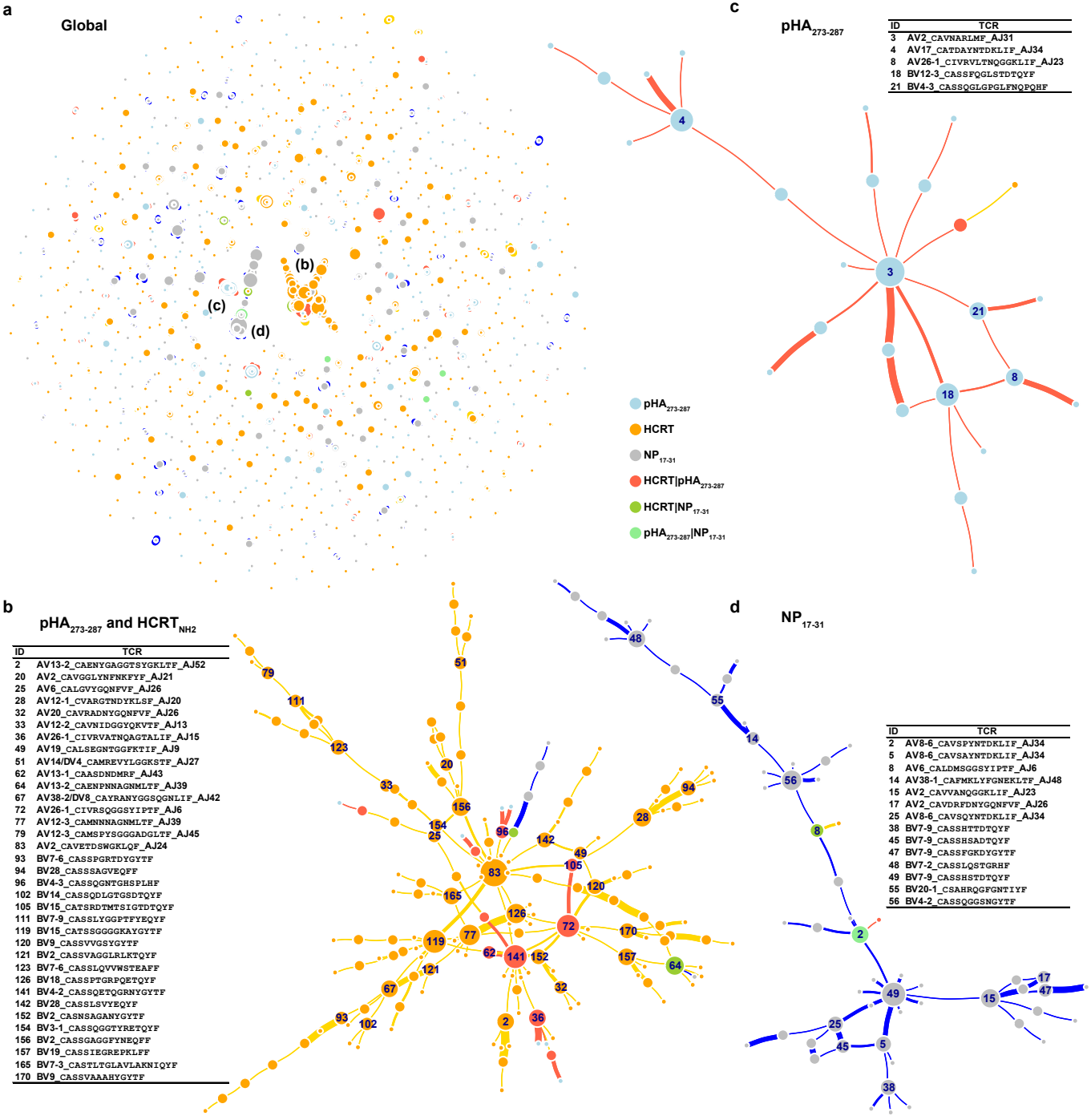

Figure 4 | Network clustering of TCR segments. **a**. Global view of network with 3 central clusters. **b**. $pHA_{273-287}$/$HCRT_{NH2}$ cluster centered around TRAJ24. **c**. $pHA_{273-287}$ only cluster. **d**. NP_{17-31} only cluster.

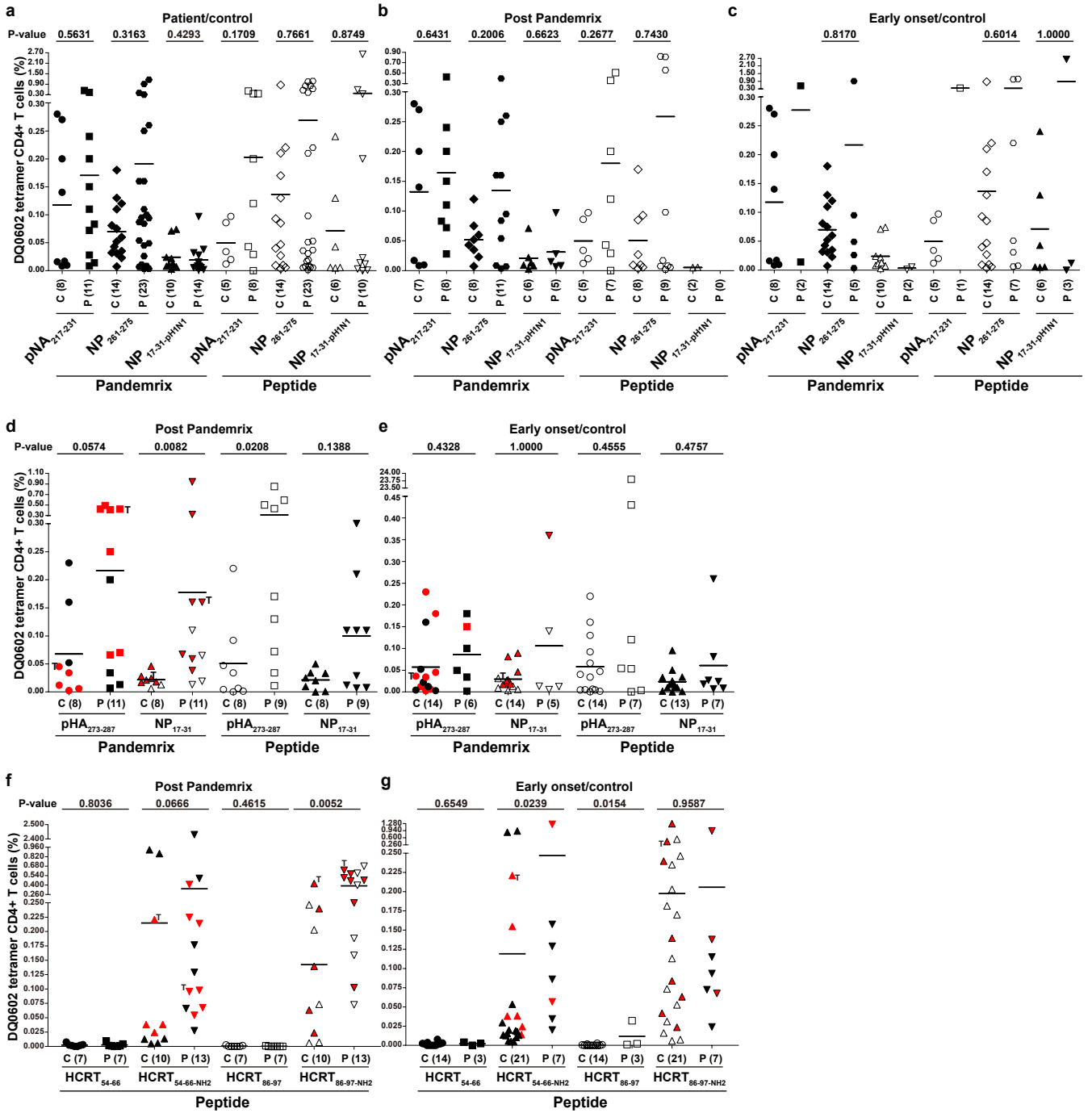

Extended Data Figure 2 | Tetramer positivity for $pHA_{273-287}$, $pNA_{217-231}$, NP_{17-31}, $NP_{17-31-pH1N1}$, $NP_{261-275}$, $HCRT_{54-66-NH2}$ and $HCRT_{86-97-NH2}$ in patients versus controls (a), including subgroup analysis of post Pandemrix cases/controls only (b,d and f) and early onset cases versus matched controls only (c, e and g). Early onset are defined as having had onset less than one year prior to blood sample. P-value is shown on top of each panel. P, patient; C, control; T, twins; Bar indicates the mean; The number of subjects tested is shown between brackets; Red, single cell TCR sequencing. For peptide and subject infomation, see Supplementary Table 1 and 9, respectively.

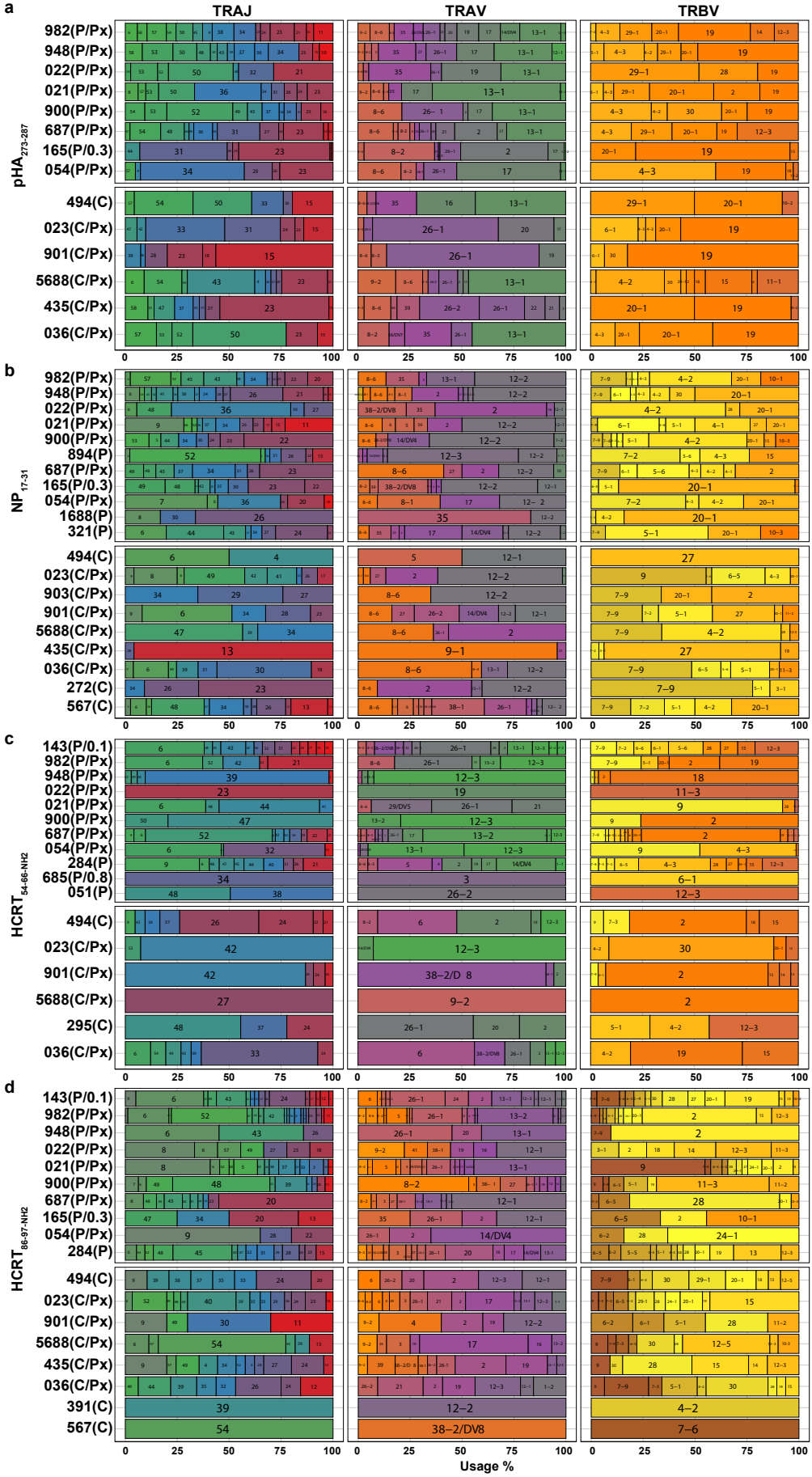

Baseline usage (%)

TRAV	TRAJ
10(2.42)	10(1.96)
1-1(0.16)	11(1.57)
1-2(0.10)	12(0.82)
12-1(1.07)	13(2.32)
12-2(0.64)	15(2.11)
12-3(1.32)	17(1.68)
13-1(1.96)	18(1.09)
13-2(0.46)	20(3.20)
14/DV4(0.65)	21(1.62)
16(1.11)	22(2.64)
17(1.32)	23(2.21)
19(2.21)	24(0.87)
2(10.79)	26(1.64)
20(1.58)	27(2.15)
21(0.37)	28(1.39)
22(0.10)	29(1.92)
24(3.88)	3(1.84)
25(7.61)	30(2.07)
26-1(6.00)	31(2.87)
26-2(0.87)	32(0.00069)
27(0.32)	33(1.60)
29/DV5(0.77)	34(3.48)
3(1.10)	35(0.88)
35(1.09)	36(1.62)
36/DV7(2.54)	37(3.96)
38-1(0.45)	38(1.16)
38-2/DV8(0.49)	39(3.02)
39(0.21)	4(2.01)
4(5.92)	40(2.66)
40(2.77)	41(1.31)
41(3.54)	42(3.29)
5(1.12)	43(2.80)
6(0.48)	44(2.52)
8-1(0.54)	45(2.54)
8-2(*29.25)	47(1.26)
8-4(*29.25)	48(2.36)
8-3(0.44)	49(4.17)
8-6(0.10)	5(2.02)
9-1(0.08)	50(0.63)
9-2(1.56)	52(3.16)
	53(2.45)
TRBV	54(2.53)
	56(0.76)
10-1(2.02)	57(1.53)
10-2(0.47)	58(1.92)
10-3(0.50)	6(2.71)
11-1(0.11)	7(0.65)
11-2(1.66)	8(1.46)
11-3(0.51)	9(2.56)
12-3(0.91)	
12-5(0.14)	
13(0.03)	
14(0.97)	
15(3.54)	
16(0.01)	
18(0.70)	
19(0.81)	
2(1.11)	
20-1(13.43)	
24-1(2.02)	
25-1(5.54)	
27(15.90)	
28(5.77)	
29-1(0.40)	
30(0.07)	
3-1(1.21)	
4-1(0.84)	
4-2(0.74)	
4-3(1.36)	
5-1(0.84)	
5-4(0.35)	
5-5(0.07)	
5-6(0.08)	
5-8(0.06)	
6-1(#14.05)	
6-2(6.60)	
6-4(1.28)	
6-5(#14.05)	
6-6(#14.05)	
7-2(6.56)	
7-3(3.33)	
7-4(0.91)	
7-6(1.13)	
7-9(1.46)	
9(0.23)	

Extended Data Figure 3 | Usage of TCR segment for main pDQ0602 tetramer ($pHA_{273-287}$ (a), NP_{17-31} (b), $HCRT_{54-66-NH2}$ (c) and $HCRT_{86-97-NH2}$ (d)) in patients and controls with corresponding mean usage (%) on blood $CD4^+$ T cells. Note that a few related chains cannot be separated by bulk sequencing but can be distinguished in single cell sequencing; these are denoted by * and # in reference population frequency. P, patient; P/Px, post Pandemrix patient; C, control; C/Px, post Pandemrix control. Interval is shown if patient is early onset (<1.0 year). TCR segment is indicated in box. For subject infomation, see Supplementary Table 9.

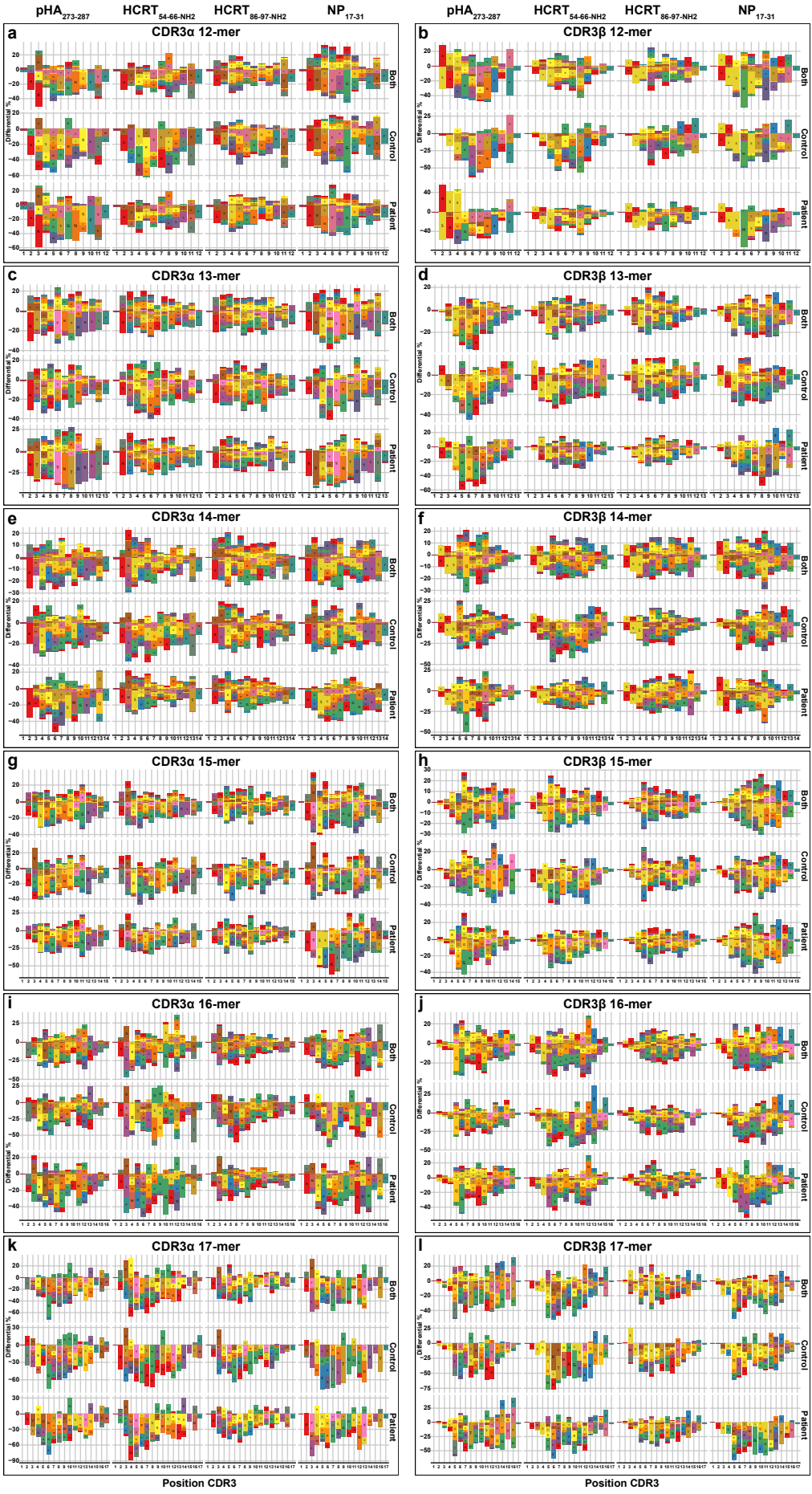

Extended Data Figure 4 | Preferential usage of specific aminoacids in tetramers versus control sequences of various lengths.

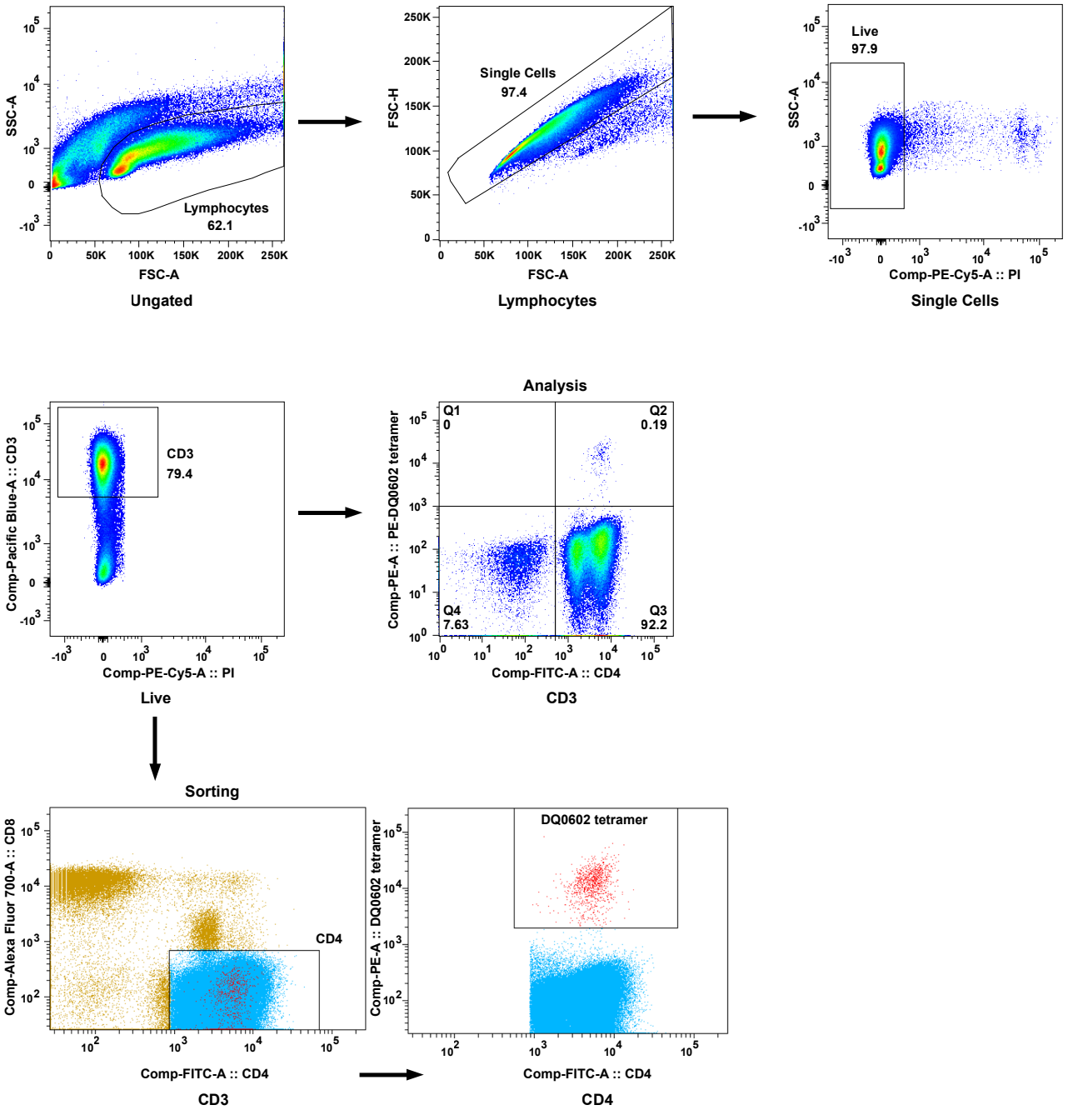

Extended Data Figure 5 | Gate strategy used for analyzing and sorting DQ0602 tetramer positive CD4⁺ T cells. % parent population is shown. Comp, compensation. A, area. H, height.